



## RESEARCH ARTICLE

# Blanket bog CO<sub>2</sub> flux driven by plant functional type during summer drought

Henk Pieter Sterk<sup>1</sup>  | Chris Marshall<sup>1</sup>  | Neil R. Cowie<sup>2</sup> | Ben Clutterbuck<sup>3</sup> | Jason McIlvenny<sup>1</sup> | Roxane Andersen<sup>1</sup>

<sup>1</sup>Environmental Research Institute, UHI North Highland, University of the Highlands and Islands, Thurso, UK

<sup>2</sup>RSPB, Centre for Conservation Science, Edinburgh, UK

<sup>3</sup>School of Animal, Rural & Environmental Sciences, Nottingham Trent University, Nottingham, UK

## Correspondence

Henk Pieter Sterk, Environmental Research Institute, UHI North Highland, University of the Highlands and Islands, Thurso, UK.  
Email: [hpsterk@gmail.com](mailto:hpsterk@gmail.com)

## Funding information

European Social Fund; Scottish Funding Council; Natural Environment Research Council, Grant/Award Number: NE/P014100/1; Leverhulme Leadership Award, Grant/Award Number: RL2019-0002; International Peatland Society - Allan Robertson Grant

## Abstract

Recent climate predictions for the United Kingdom expect a nationwide shift towards drier and warmer summers, increasing the risk of more frequent and severe drought events. Such shifts in weather patterns impede functioning of global peatlands, especially rare intact blanket bogs abundant in Scotland and representing nearly a quarter of the UK's soil carbon. In this in situ study, carbon dioxide (CO<sub>2</sub>) fluxes from dominant peatland plant functional types (PFTs) such as *Sphagnum* spp., graminoids, ericoids and other key cover types (i.e., pools and bare peat) were measured and compared across upland and low-lying blanket bog margins and centres, immediately before and during a summer drought in 2018, and over the subsequent year. During that period, most sites acted as net sources of CO<sub>2</sub> to the atmosphere. Our results showed that net ecosystem exchange (NEE) was limited by water availability during the drought, with ericoid shrubs showing the highest drought resilience, followed by graminoids (which were still limited in GPP in 2019) and *Sphagnum* mosses. Diverging NEE estimates were observed across centre and margin areas of the blanket bogs, with highest variability across the upland site where signs of active erosion were visible. Overall, our study suggests that estimating growing season carbon fluxes from in situ peatland PFT and cover types can help us better understand global climate change impacts on the dynamics and trajectories of peatland C cycles.

## KEYWORDS

carbon dioxide, ecosystem respiration, gross primary productivity, net ecosystem exchange, peatland

## 1 | INTRODUCTION

Current European climate models indicate a shift towards drier and warmer summers over the 21st century (Chan et al., 2018; Chan et al., 2020). These climatic changes are predicted to increase the intensity, frequency and duration of drought periods across the UK (Forzieri et al., 2014; Grillakis, 2019), driven largely by reduced precipitation and increased evapotranspiration (Berg & Sheffield, 2018;

Roudier et al., 2016). Although in Scotland, mean annual rainfall over the past decade (2008–2017) has increased by 11% compared to the long-term mean (1961–1990; UK Climate Projections 2018 (UKCP18) [Lowe et al., 2018]). However, climate models also indicate that parts of Scotland will experience increasingly hotter and drier summers through the 21st century.

Such changes in precipitation patterns can have direct (i.e., changing water availability and evapotranspiration rates) or

This is an open access article under the terms of the [Creative Commons Attribution](https://creativecommons.org/licenses/by/4.0/) License, which permits use, distribution and reproduction in any medium, provided the original work is properly cited.

© 2022 The Authors. *Ecohydrology* published by John Wiley & Sons Ltd.

indirect (i.e., altered surface water runoff or lateral drainage) effects on ecosystem distribution and functioning (Radu & Duval, 2018). Quantifying these effects is needed to improve models that include long-term datasets or mean annual variable values to predict future climate, especially since these models often fail to acknowledge the extreme events (Gallego-Sala et al., 2010). This is particularly relevant for ecosystems whose present bioclimatic space is likely to contract under future climate change scenarios, such as northern peat bogs (Chaudhary et al., 2020) and within the Scottish context, blanket bogs (Clark et al., 2010; Gallego-Sala & Colin Prentice, 2013).

To improve our understanding of the consequences of extreme events, such as droughts, on carbon cycling in blanket bog, one approach is to characterise the individual responses of key plant functional types (PFTs). In blanket bogs, key PFTs consist of ericoid shrubs, graminoids (e.g., sedges), herbs, *Sphagnum* spp. and other mosses (Berger et al., 2018; Laine et al., 2016). Previous long-term studies using a PFT approach have demonstrated that peatland vascular PFTs (graminoids and shrubs) control gaseous methane emissions (Armstrong et al., 2015; Goud et al., 2021; Robroek et al., 2015), while increased *Sphagnum* moss coverage reduces fluvial dissolved organic carbon (DOC) effluxes (Dunn et al., 2016). Furthermore, peatland carbon cycling may be constrained by ericoid shrubs presence, as increased gross CO<sub>2</sub> fluxes from graminoids were observed during selective removal experiments of key PFTs, that is, ericoid shrubs (Ward et al., 2009). A climate-driven shift in PFT composition could therefore influence total C sequestration in UK blanket bogs. However, these manipulative studies do not capture the immediate, short-term effects of actual drought-induced stress on greenhouse gas (GHG) emissions, which combine in situ reduced water availability and higher temperatures.

To date, the short-term effect of drought stress on C sequestration in peatlands has primarily been measured through mesocosm experiments (Dieleman et al., 2015; Fenner & Freeman, 2011; Kuiper et al., 2014). While useful to understand mechanisms and controls on PFT-response to drought, these laboratory-controlled settings may not fully reflect in situ responses, as they cannot account for local variations in microhabitat condition or topographic setting, which may influence GHG fluxes during periods of drought. For example, *Sphagnum* species located in higher elevation areas (i.e., mountains) suffer a stronger negative effect on CO<sub>2</sub> uptake during periods of increased temperature (Gerdol & Vicentini, 2011). *Sphagnum* spp. are one of the key peat-forming taxa in blanket bog, owing to their capacity to hold water and intrinsic properties (Bengtsson et al., 2016; Turetsky, 2003). However, *Sphagnum* spp. are known to be vulnerable to prolonged drought periods, as they are not well adapted to high temperatures and low precipitation rates (Bragazza, 2008; Gerdol & Vicentini, 2011; Van Breemen, 1995). Lowered water table depths in blanket bogs could cause a shift from *Sphagnum* spp. to other moss species that are better adapted to prolonged periods of droughts such as *Polytrichum* spp. (Potvin et al., 2014) and *Racomitrium lanuginosum* (Lindsay, 2010). Such change in vegetation would have potential consequence for long-term C uptake. Identifying the drivers and thresholds in atmospheric and edaphic conditions beyond which different

PFTs shift from net CO<sub>2</sub> sinks to sources is therefore essential to improve our understanding of the potential consequences of droughts on blanket bog C dynamics.

In 2018, a persistent high-pressure system resulted in a period of drought across Europe between April and October (Buras et al., 2020; Hari et al., 2020). In Scotland, the months of May, June and July 2018 were nearly 2°C warmer than the long-term monthly mean (1981–2010) and received only between a quarter and a half of the long-term mean monthly ( $64 \pm 15$  mm compared to  $86 \pm 7$  mm) rainfall (Supporting information, Figure S2).

This provided an opportunity to measure the immediate and short-term (1 year post drought) effects of the 2018 drought on CO<sub>2</sub> emissions from blanket bog sites in Scotland. For this study, we first aimed to compare in situ small-scale CO<sub>2</sub> fluxes from a range of PFTs (*Sphagnum* spp., graminoids, ericoids and other mosses) and key blanket bog features (pools and bare peat) in two near-natural blanket bogs in Scotland. We examine empirical relationships between CO<sub>2</sub> fluxes and edaphic and atmospheric conditions to derive modelled annual CO<sub>2</sub> balance for the dominant PFTs during the 2018 drought and the following growing season of 2019. We report on variation observed between microtopes (margins and centre) and topographical setting (upland and lowland). We hypothesised that CO<sub>2</sub> fluxes would vary amongst the dominant blanket bog PFTs (*Sphagnum* spp., ericoids and graminoids) because of their functional traits; notably that they would vary in their productivity during drought conditions, and potentially during recovery period in the post-drought year. Differences in fluxes between the topographic settings are expected to relate to water availability variations during the sampling period.

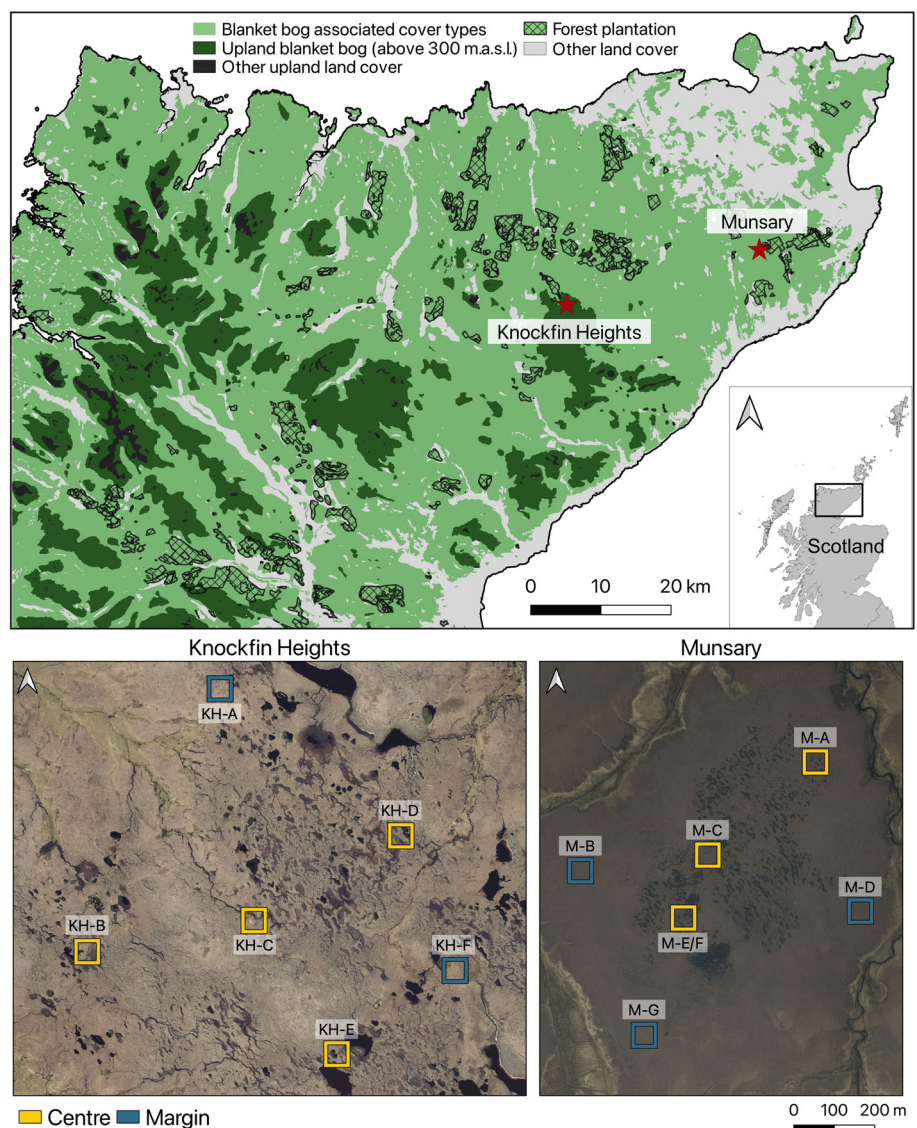
## 2 | MATERIALS AND METHODS

### 2.1 | Site description

The study was conducted at two blanket bogs in northern Scotland, part of the Flow Country peatlands (Andersen et al., 2019; Lindsay et al., 1988): RSPB Forsinard Knockfin Heights and Plantlife Munsary Peatlands (referred to as Munsary hereafter; Figure 1). Knockfin Heights is an upland site (58°19'07.7" N, 3°48'22.8" W, 340–440 m. a.s.l.) characterised by blanket bog and wet heath vegetation showing signs of active erosion (Hancock et al., 2018) and with peat depths ranging from 0.5 to 4.3 m (Avercamp et al., 2021). Ericoid shrub species include *Calluna vulgaris* L. and *Erica tetralix* L., with a graminoid cover dominated by *Eriophorum angustifolium* L., *Trichophorum germanicum* L. and *Carex panicea* L. Common mosses include *Sphagnum capillifolium*, *Sphagnum cuspidatum*, *Sphagnum fuscum* and *R. lanuginosum*. *E. angustifolium* colonised peat hags and dry pools in wetter areas.

The lower altitude site Munsary (58°23'49.0" N, 3°20'26.5" W, approximately 100 m.a.s.l.) is located 30 km to the east of Knockfin and comprises low-lying blanket bog with peat depths between 2 and 5 m (Marshall et al., 2022). The mire expanse contains a wide range of micro-topographic elements such as hummock and hollows, with an

**FIGURE 1** Top: location of study sites in the upland (>300 m.a.s.l.) and low-lying blanket bogs in the Flow Country, northern Scotland. Map is derived from the Carbon and Peatland map (SNH, 2016), showing all features associated with blanket bog habitat and soil types. Bottom: distribution of sampling plots (100 × 100 m, after Marshall et al., 2022) of different microtope positions across the upland site Knockfin Heights and low-lying site Munsary, overlain on a modified greyscale ©2022 Bing Maps satellite image for reference to highlight plot distribution



extensive pool system in the centre (Smart, 1982). *Sphagnum* spp. include *Sphagnum papillosum*, *Sphagnum medium*, *Sphagnum austini* and *S. capillifolium*, while other bryophytes include *Polytrichum commune* and *R. lanuginosum*. For vascular species, *C. vulgaris*, *E. angustifolium* and *Eriophorum vaginatum* are abundant, together with *T. germanicum* and *Narthecium ossifragum*. Agricultural drains, historically cut in one area close to the southwestern margin of the site, were blocked with peat dams and plastic piling in the early 2000s.

At each site, six replicated sampling plots were set up, with no more than one sampling plot within each 100 × 100 m subsite to capture variation between different margin and centre microtopes (Figure 1) as identified by Marshall et al. (2022). Margin plots are associated with generally stiffer peat and are situated near the boundaries of the blanket bog expanse on the site (i.e., streams adjacent to Munsary and erosion gullies at Knockfin Heights). Centre microtope sites are found in the central, wetter and deeper peat areas, often with pool systems. At each plot, after an initial high-level (PFT and dominant cover type) vegetation survey in November 2017, collars were

installed around three key peatland PFTs (*Sphagnum* spp., graminoids and ericoids) and where present, on lichen (*Cladonia* spp.), other mosses (*Pleurozium schreberi*), bare peat (natural and anthropogenic originated erosion [Hancock et al., 2018]) and pools (Figure 2) (Supporting information, Table S1). In order to allow for efficient CO<sub>2</sub> flux measurements and site-specific environmental condition monitoring, all collars were installed within an area of 5 × 5 m that was representative for the margin or centre microtope at the plot.

## 2.2 | Flux chamber measurements

Between April–November 2018 and May–October 2019, CO<sub>2</sub> concentration-change was measured on 19 occasions using a mobile infrared gas analyser (IRGA; EGM-4, PP System) attached to a mobile cylindrical non-steady-state chamber (diameter of 19.2 cm, height 20 cm, volume 5.8 L) sealed to the ground-based collars. A dome-shaped floating chamber with an air volume of 4 L was used to

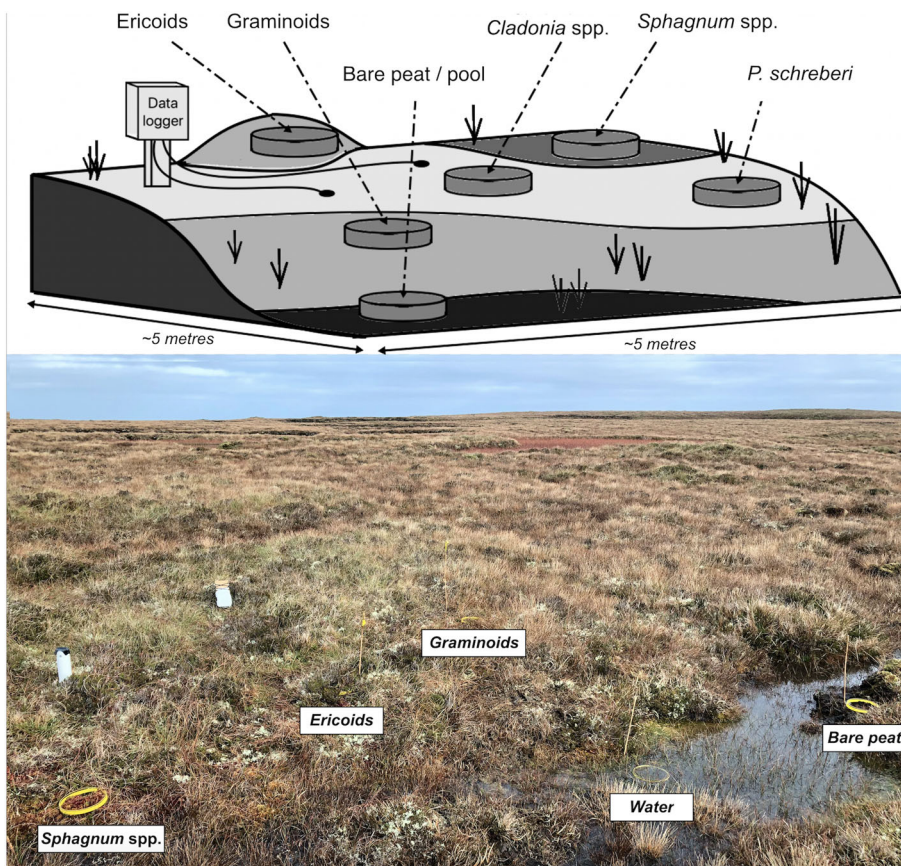


**FIGURE 2** Top: schematic example of collar set-up, indicating plant functional type (PFT) variability within a plot (note: actual PFT distribution and occurrence vary amongst plots). Bottom: margin plot (KH-A) at Knockfin Heights with water level logger (left), soil temperature and water content logger and five collars placed at dominant PFTs and key blanket bog features

measure pools. A fan was installed inside all the chambers to increase homogeneity of the sampled air during deployment.

To estimate ecosystem respiration ( $R_{\text{eco}}$ ; total  $\text{CO}_2$  respiration from plants, roots and soil microbes per unit ground area) and net ecosystem exchange (NEE) fluxes (the  $\text{CO}_2$  respiration minus  $\text{CO}_2$  fixation of the plant flux per unit ground area), the IRGA recorded  $\text{CO}_2$  concentrations at an interval of 1.6 s (Sterk et al., 2019) from the moment the chamber was put on the collar until the  $\text{CO}_2$  concentrations stabilised, which took on average 2.65 min (between on average 2.88 min for *Sphagnum* spp. and 2.56 min for graminoids). For  $R_{\text{eco}}$  measurement, the chamber was covered with a reflective shroud (i.e., dark chamber) that was removed for NEE measurement (clear chamber). Between the two measurements, the chamber was removed from the collar and vented.

### 2.3 | Ancillary environmental measurements

To record environmental data between sampling, at each plot, data were collected at 30-min intervals for volumetric soil water content (10-HS S-SMD-M005, Onset), soil temperature (S-TMB-M002, Onset), water level and temperature (U20L-004, HOBO), precipitation (S-RGF-M002, Davis), atmospheric pressure (S-BPB-CM50, Onset) and photosynthetic active radiation (PAR, S-LIA-M003, Tempcon) from September 2017 until November 2019. Due to deer damage to some of the dataloggers on Knockfin Heights, gaps in PAR and

precipitation data are present in the second half of 2019. Precipitation data for Northern Scotland were obtained from the Met Office (Met Office, 2020) to enable comparison of monthly rainfall with the long-term mean (1981–2010) for both sites. In addition to automated measurements collected at the plot level, soil temperature (EcoTemp thermometer; ETI Ltd, Worthing, Surrey, UK and HI 955502 Digital Thermometer; Hanna Instruments, Bedfordshire, UK), soil water content (HH2-Theta Probe, type ML2x; Delta-T Devices, Cambridge, UK) and average PAR (MQ-100; apogee instruments, Logan, Utah, USA) were recorded manually for all chamber measurements. All recorded soil parameters were measured at 5 cm depth. The EGM-4 also stores relative humidity (RH) and air temperature during deployment. Weather conditions and comments on on-site disturbances (e.g., deer trampling near/on collars) were also noted.

### 2.4 | Flux calculations

#### 2.4.1 | In situ fluxes

All  $\text{CO}_2$  fluxes ( $\mu\text{mol CO}_2 \text{ m}^{-2} \text{ s}^{-1}$ ) were calculated by applying a linear regression or quadratic regression model in Python (version 3.6.3) using the *statsmodels* package (Seabold & Perktold, 2010). The convention of a negative rate indicating an uptake of  $\text{CO}_2$  (i.e., sink) and positive rates for net emissions (source) has been adopted. The  $\text{CO}_2$  concentration (ppm) data were first checked for outliers with an

automated moving-window analysis to subsample the full dataset, retaining as many data points as possible, while omitting concentration outliers. Outliers include anomalously high, low or stable concentrations at the start or end of a measurement, indicating response-lag or equilibrium conditions, respectively (Pirk et al., 2016). Removing these points retained a sufficient period for actual flux calculations where the true rate is identified in the moving-window analysis (Supporting information, Figure S1).

When concentration flux is low, all data points are kept in the subsequent subset analysis, indicative of a net zero rate. A subset of data with the best linear model quality parameters was selected: that is, highest  $r^2$ , lowest normalised root mean squared error (NRMSE) and highest Nash Sutcliffe efficiency coefficient (E). The subset was subsequently used for both linear and quadratic regression analyses, following the flux calculation procedures used by the IRGA (EGM-4, PP Systems). The rates were calculated using a discrete function (Parkinson, 1981; Widén & Lindroth, 2003):

$$F_i = \frac{(C_i - C_0) \times V}{t_i \times A} \quad (1)$$

where the concentration linear flux rate  $F_i$  is a function of the change in concentration  $C$  at time  $t_i$ , the volume of the chamber  $V$  and the horizontal area of the chamber  $A$ . This function contains the linear equation used to determine flux rates, before adjusting for chamber dimensions and water vapour concentration changes:

$$\frac{dC}{dT} = b \quad (2)$$

where change in concentration  $C$  is a constant linear function over time  $T$ .

Non-linear behaviours of both NEE and  $R_{\text{eco}}$  fluxes have been recognised for chamber measurements (Kutzbach et al., 2007; Murphy et al., 2014; Pirk et al., 2016), resulting in the use of a quadratic function to estimate the  $\text{CO}_2$  flux:

$$\frac{dC}{dT} = b + 2cT \quad (3)$$

where the change in concentration  $C$  over time  $T$  is constant at  $T = 0$ , resulting in a linear flux rate value that is not influenced by the derivative of the observer effect ( $2cT$ ) (Wagner et al., 1997).

Model fit statistics were assessed to determine whether observed flux estimates fit a linear or quadratic function best and hence better represented ambient flux prior to measurement start. For the linear flux estimates, the model's coefficient of determination ( $r^2$ ) generally provides a robust representation of the data when close to 1 (being a perfect linear regression line). Since higher-order polynomial regressions (i.e., the quadratic function) are not properly described by  $r^2$ -values, they are compared using  $r^2_{\text{adj}}$ -values using the *statsmodels Ordinary Least Squares* function. Both linear and quadratic rates are calculated, and model parameters are stored for the following model-

selection steps. Subsequently, rates are corrected for an increase of water vapour concentrations as dilution by water molecules can significantly reduce  $\text{CO}_2$  flux estimates (Matsuura et al., 2011).

Confident linear rates are assumed for all NEE and  $R_{\text{eco}}$  fluxes based on a linear model with  $r^2_{\text{adj}}$ -values  $>0.85$  (Huttunen et al., 2002; Silva et al., 2015) (Supporting information, Figure S1). Additionally, linear rates with  $r^2_{\text{adj}}$ -values  $>0.75$  are accepted (Strack et al., 2016) unless a concentration change of more than  $\pm 2$  ppm of the initial measurement level was observed. The quadratic model rate was used when quadratic  $r^2_{\text{adj}}$ -value exceeded 0.75, and the  $r^2_{\text{adj}}$ -value of the linear rate is lower than 0.75, together with a  $r^2$ -value  $\neq 0$  of the moving-window analysis (indicating an absolute rate, greater than zero:  $|b| \gg 0$ ).  $R^2_{\text{adj}}$ -values of 0 for linear rates accompanied with a  $\pm 2$  ppm range (indicative of low fluxes) are also accepted.

In total, 3% of the NEE and  $R_{\text{eco}}$  fluxes were omitted from the dataset, and all other fluxes are best described by a linear rate. Depending on the final flux type, the value of  $b$  from either the linear [2] or quadratic function [3] was subsequently used to define NEE and  $R_{\text{eco}}$  fluxes at time of the measurement. As the NEE chamber deployment immediately followed the dark  $R_{\text{eco}}$  flux measurement, gross primary production (GPP; rate of  $\text{CO}_2$  uptake through photosynthesis) was calculated as the difference between the two measurements.

## 2.4.2 | Potential maximum photosynthesis ( $P_{\text{max}}$ )

Since all GPP fluxes (derived from  $\text{NEE} - R_{\text{eco}}$ ) were measured under varying light conditions,  $P_{\text{max}}$  was calculated for the dominant PFTs across both growing seasons using the Michaelis-Menten function (Laine et al., 2016):

$$GPP_{ghi} = P_{\text{max}ghi} \times \left( \frac{PAR_{ghi}}{k_{ghi} + PAR_{ghi}} \right) \quad (4)$$

with  $P_{\text{max}}$  as the potential maximum rate of photosynthesis ( $\mu\text{mol CO}_2 \text{ m}^{-2} \text{ s}^{-1}$ ), the half saturation constant  $k$  and the PAR measurement associated with the GPP flux during year  $i$ , on collar  $h$  at site  $g$ .

A non-linear least-squares (nls) model was used to estimate  $P_{\text{max}}$  and  $k$  coefficients across the data, grouped by collar and year (function *nlsList* package *nlme* [Pineiro et al., 2020] in R version 3.6 [R Core Team, 2014]). Subsequently, negative  $k$  coefficient estimates are omitted, along with the paired  $P_{\text{max}}$  values; negative light levels at which half of  $P_{\text{max}}$  is reached are not used in further analyses. Only two extreme  $P_{\text{max}}$  estimations ( $-81$  and  $-119 \mu\text{mol CO}_2 \text{ m}^{-2} \text{ s}^{-1}$ ) were left out due to their very high  $k$  estimates ( $\gg 30,000 \mu\text{mol m}^{-2} \text{ s}^{-1}$ ). A total of 34  $P_{\text{max}}$  and  $k$  coefficients of the collars are then used to describe functioning of the different PFTs between years, sites and microtopography.

## 2.5 | Estimation of growing season fluxes

The number of flux estimates allows for modelling of hourly GPP and  $R_{\text{eco}}$  rates across the sampling periods in 2018 and 2019. Soil

temperature, water table and PAR can be used to predict diurnal variability of fluxes (Wilson et al., 2016) and offer an effective way to model annual NEE based on flux chamber measurements (Huth et al., 2017; Swenson et al., 2019). To be able to compare the carbon sequestering functioning to similar blanket bogs and peatlands, carbon fluxes are converted to  $\text{g C-CO}_2 \text{ m}^{-2} \text{ h}^{-1}$ . The focus was on *Sphagnum* spp., graminoids and ericoids, which had the highest number of measurements available for this modelling. Furthermore, to assess both temporal and spatial PFT flux behaviour, field measurements are divided based on site and microtope. To allow for appropriate site- and microtope-specific GPP and  $R_{\text{eco}}$  estimations, each subset was accompanied by their respective hourly average soil temperature ( $^{\circ}\text{C}$ ), water level (cm below surface) and average PAR ( $\mu\text{mol m}^{-2} \text{ s}^{-1}$ ).

For modelling of hourly GPP and  $R_{\text{eco}}$ , a range of variations of empirical non-linear regression models, based on work by Swenson et al. (2019), are tested using the *nls.multstart* package (Padfield & Matheson, 2018) in R. Across the three PFTs, two sites and two microtope categories (Equation 5) best described the variance in the estimated in situ GPP fluxes, based on the sum of squares of the residuals and  $r^2$  values:

$$\text{GPP} = -\left(a + c * \sin\left(\frac{J + 215}{365} * 2\pi\right)\right) * \frac{\text{PAR}}{\text{PAR} + b} * (1 + T_{\text{soil}} * b) * (1 + W_{\text{level}} * e) \quad (5)$$

where PAR is the photosynthetic active radiation ( $\mu\text{mol m}^{-2} \text{ s}^{-1}$ ),  $T_{\text{soil}}$  is the soil temperature ( $^{\circ}\text{C}$ ),  $W_{\text{level}}$  is the water level (cm), which are all measured empirically. In the empirical model, Julian day of the year ( $J$ ) was used to account for any seasonal variability of plant phenology, such as changes in green leaf area (Wilson et al., 2007) and model parameters  $a$ ,  $b$ ,  $c$ ,  $d$  and  $e$  are specific to each PFT-site-microtope combinations (3 PFTs  $\times$  2 sites  $\times$  2 microtopes = 12 individual models) (Supporting information, Table S4).

A similar non-linear regression empirical approach was used to fit measured  $R_{\text{eco}}$  fluxes:

$$R_{\text{eco}} = (a + b * W_{\text{level}}) * \exp\left(c * \left(\frac{1}{283.15 - 227.13} - \frac{1}{T_{\text{soil}} - 46.02}\right)\right) \quad (6)$$

where model parameters  $a$ ,  $b$  and  $c$  are unique to a PFT-site-microtope combination and the  $T_{\text{soil}}$  and  $W_{\text{level}}$  are the same as Equation (5) (Supporting information, Table S5).

Using both functions, subsets of the environmental data are used to predict hourly GPP and  $R_{\text{eco}}$  for the months covering the sampling period (April 1st–November 31st) for both years to capture the majority of the growing season. As with the in situ flux processing, all positive GPP (3.9%) and negative  $R_{\text{eco}}$  (1.2%) estimates were omitted from the dataset. Complete diurnal measurements were not obtained, and therefore, only daytime fluxes are modelled; the daytime (PAR > 25  $\mu\text{mol m}^{-2} \text{ s}^{-1}$ ) flux estimates, accounting for 53% of the modelled GPP and  $R_{\text{eco}}$ , are used for growing season NEE estimates (NEE = GPP +  $R_{\text{eco}}$ ). In order to obtain a confidence range of

predicted fluxes, the residual standard error (RSE) of each model (predicted values are converted back to  $\mu\text{mol CO}_2 \text{ m}^{-2} \text{ s}^{-1}$  to allow for direct comparison with the in situ measurements) was used to calculate lower and upper estimates for the fluxes and subsequently the cumulative GPP and  $R_{\text{eco}}$ , as well as NEE.

## 2.6 | Statistical analysis

### 2.6.1 | Comparison of in situ NEE, $R_{\text{eco}}$ , GPP and $P_{\text{max}}$ fluxes

All statistical analyses were conducted using R (version 3.6) and the most recent versions of the packages at time of writing. Linear mixed-effects models (LMEMs) (function *lmer* from package *lme4* [Bates et al., 2015]) with plot ID as a random effect were used to test whether NEE,  $R_{\text{eco}}$  and GPP are different between PFTs and ground cover types, both within and between both years and between sites (upland vs. low-lying). For each LMEM, an ANOVA was applied to check the contribution to the models' variances for each fixed effect (ANOVA type III, function *anova* from *stats* package [R Core Team, 2014]). PFTs and ground cover types significantly contributed to the variance ( $p < 0.001$ ) of the three LMEMs (NEE,  $R_{\text{eco}}$  and GPP). Even though the interaction between PFTs and years is not significantly contributing to the variance in the  $R_{\text{eco}}$  LMEM, the interaction factor was kept in all subsequent post-hoc tests as it is a significant contributor in the NEE and GPP models ( $p < 0.05$ ). A pairwise comparison test (function *glht* from *multcomp* package [Hothorn et al., 2008]) was applied to each LMEM using a post hoc (Tukey) analysis to investigate differences in marginal means for all 'PFTs and ground cover - Year' pairs and was accompanied by letter-based representations of significantly different marginal means ( $p < 0.05$ ) (function *cl* from *multcomp* package).

Only  $P_{\text{max}}$  estimates of *Sphagnum* spp., graminoids and ericoids were used for testing differences between years, sites and microtopography. Small sample sizes ( $n < 30$ ) of *P. schreberi* and *Cladonia uncialis/impexa*-mix impeded reliable coefficient estimates and were excluded together with the other ground cover types (i.e., pools and inundated/dry bare peat). Means of yearly  $P_{\text{max}}$  estimates per collar were compared between *Sphagnum* spp., graminoids and ericoids using an LMEM with collar ID as a random effect (function *lmer* package *lme4*). A complex model (with the fixed-effects PFT, year, sites and microtopes) was fitted and compared to models with univariate models and interactions (i.e., PFTs across years). For all model configurations—including and excluding some predictors—the Akaike information criterion (AIC) was calculated (Burnham & Anderson, 2004). The most complex model has the best fit (AIC = 175.08,  $\text{df} = 23$ ), but the interaction model of PFT and year shows higher  $F$ -values (indicating that the variation amongst the means is less likely to be caused by chance) for both fixed effects and their interaction (AIC = 188.44,  $\text{df} = 8$ ). To test for differences of mean  $P_{\text{max}}$  for each PFT and year, a post-hoc (Tukey) analysis was used to compare estimated marginal means (function *emmeans* and *glht* from packages *emmeans* [Lenth et al., 2020] and *multcomp*).

## 2.6.2 | Environmental control on fluxes

To investigate the controls of the environmental conditions on in situ NEE,  $R_{\text{eco}}$  and GPP flux measurements for the three dominant PFTs (graminoids, ericoids and *Sphagnum* spp.) in 2018 and 2019, LMEMs were used. From the environmental data, daily minimum, maximum and range of soil temperature and daily mean and range of water content and water level for all individual plots were extracted from the 30-min interval dataset. To ensure data reliability, NEE,  $R_{\text{eco}}$  and GPP rates were matched with environmental data recorded in their respective plots from the time of chamber deployment. Subsequently, all numerical predictors were standardised to their z-score to allow for better comparison between model effects (Nakagawa & Schielzeth, 2010). Strong linearly correlated variables (all rolling-averages, daily sum of PAR and water temperature) were omitted after visual inspection and guided by Pearson's  $r$  and their significance levels ( $p < 0.01$ ).

For each PFT and ground cover type, a single complex model was built using all environmental variables as fixed effects, including categorical variables for plot microtope and year. In all models, categorical plot and site variables were included as nested random effects to allow for control on variation in location and plots within their respective sites. Additionally, a non-nested categorical *Year* variable was added to the models as plots and sites remained the same for both years. Since the influence of the extreme summer drought of 2018 is of primary interest, the variable *Year* was kept in all the models as a fixed effect, and *Drought* was excluded (as it is associated with the main sampling period in 2018). Individual model selection was based on lowest AIC, for a model including *Year* as one of the fixed effects. Another goodness-of-fit parameter used for model selection is conditional r-squared values, indicating how much model variance is explained by the complete model including both fixed and random effects (Nakagawa & Schielzeth, 2013) (function *performance* from package *performance* [Lüdecke et al., 2020]). Furthermore,  $p$ -values for fixed effects are used as a guide to model selection: Simple models (<3 predictors) often include a higher number of fixed effects that significantly contribute to model variance compared to more complex models.

## 2.6.3 | Generalised additive mixed-effect models

To overcome any potential nonlinearity of environmental variation throughout the year that would limit the usability of LMEMs, generalised additive mixed-effects models (GAMMs) were used to test interactive effects of changing edaphic and atmospheric conditions. In contrast to the LMEM approach, variables are not scaled to allow for direct interpretation of the model output and seasonality of environmental conditions (i.e., for temperature and water content) and applied smooth terms to the variables to run the GAMMs using the *mgcv* package (Wood, 2017) in R. Model construction was similar to LMEM: Complex multivariate models are fitted to the NEE,  $R_{\text{eco}}$  and GPP fluxes, and a stepwise removal of least-significant effects was chosen for the model selection procedure. The final model is chosen based on visual inspection (function *gam.check* in *mgcv*) and through

model summary statistics (i.e., restricted maximum likelihood [REML] and adjusted r-squared values). The small number of observations and prominent 'dominant' flux drivers (describing more of the variance in the flux measurements compared to other effects) resulted in the selection of bivariate GAMMs to highlight the most significant covariates of flux variability for *Sphagnum* spp., graminoids and ericoids. To test the interactive effect of the covariates (e.g., temperature and water content), an interactive term  $t2$  (*temperature* and *water content*) was used in all models, as univariate models performed poorer when using smooth constructions in the GAMMs. In each model, site location, plot and year were used as random effects to allow for individual slope estimates across both sites; microtope was left out as both fixed and random effects, as it did not improve the model fit criteria significantly either way. All models were fitted using the *gam4V* function from the *mgcViz* package (Fasiolo et al., 2020), as it can handle both nested and crossed random effects ( $1|\text{site/plot} + (1|\text{year})$ ) (Wood, 2019) and allows for greater graphical freedom when plotting the output. Visual interpretations of the model output were produced with *ggplot2* (Wickham et al., 2019), and covariate interactions were presented as fitted effects of NEE,  $R_{\text{eco}}$  and GPP fluxes (Supporting information, Table S6).

## 2.7 | Comparing NEE

The growing season NEE estimates ( $\text{g C-CO}_2 \text{ m}^{-2} \text{ y}^{-1}$ ) were contrasted with results from previous work by comparing sites, across a range of peatland types, summarised by Swenson et al. (2019). Both flux chamber and eddy covariance (EC) measurements were included to provide a comprehensive overview of  $\text{CO}_2$  balance estimates across boreal and temperate peatlands. These peatland types include (near-)natural blanket bogs; other bogs (such as oligotrophic and ombrotrophic peatland sites that also have not been impacted by any disturbances); a range of poor fens; sites with bare peat (resulting from peat harvesting or erosion); and peatlands which have undergone some kind of restoration management (e.g., drain-blocking or re-wetting). As both Knockfin Heights and Munsary are identified as 'near-natural' blanket bogs, comparisons with afforested sites (including restoring sites after tree-felling), rich-fens and tropical peatlands have been excluded. Mean annual water table was used to compare between sites and years as this aspect reflects annual hydrological conditions on a site and microtope scale and can be linked to annual NEE estimates (Gažovič et al., 2013; Helfter et al., 2015; Kritzler et al., 2016).

## 3 | RESULTS

### 3.1 | Environmental conditions

Monthly precipitation at both sites in 2018 was lower than the long-term (1981–2010) monthly mean of Northern Scotland, particularly over a period of drought (24 May 2018–17 September 2018)

(Supporting information, Figure S2). The precipitation deficit was not limited to the drought period as lesser precipitation (38%–79%, 35%–83% and 29%–76%) was recorded across the spring, summer and autumn months, respectively. Mean summer (June–August) air temperatures recorded for Northern Scotland in 2018 (13.1°C) and 2019 (12.8°C) were comparable, although mean daily maximum temperatures recorded over these months were almost 1°C higher in 2018 (17.0 vs. 16.3°C) (Supporting information, Table S3, including climate means for weather stations Altnaharra [~35 km west of Knockfin

Heights] and Wick [~16 km east of Munsary]). Mean soil temperature at both sites (January–October) was lower in 2018 than in 2019 (7.9 vs. 8.9°C for Munsary; 6.6 vs. 6.9°C for Knockfin Heights).

The precipitation deficit observed in 2018/2019 impacted soil water content and water level distributions across both years. At Munsary, the decline in water content was greater in margin sites compared to centre plots during the drought period (Figure 3e). At Knockfin Heights, higher water content was recorded in the margin sites compared to centre plots after the drought period. Munsary

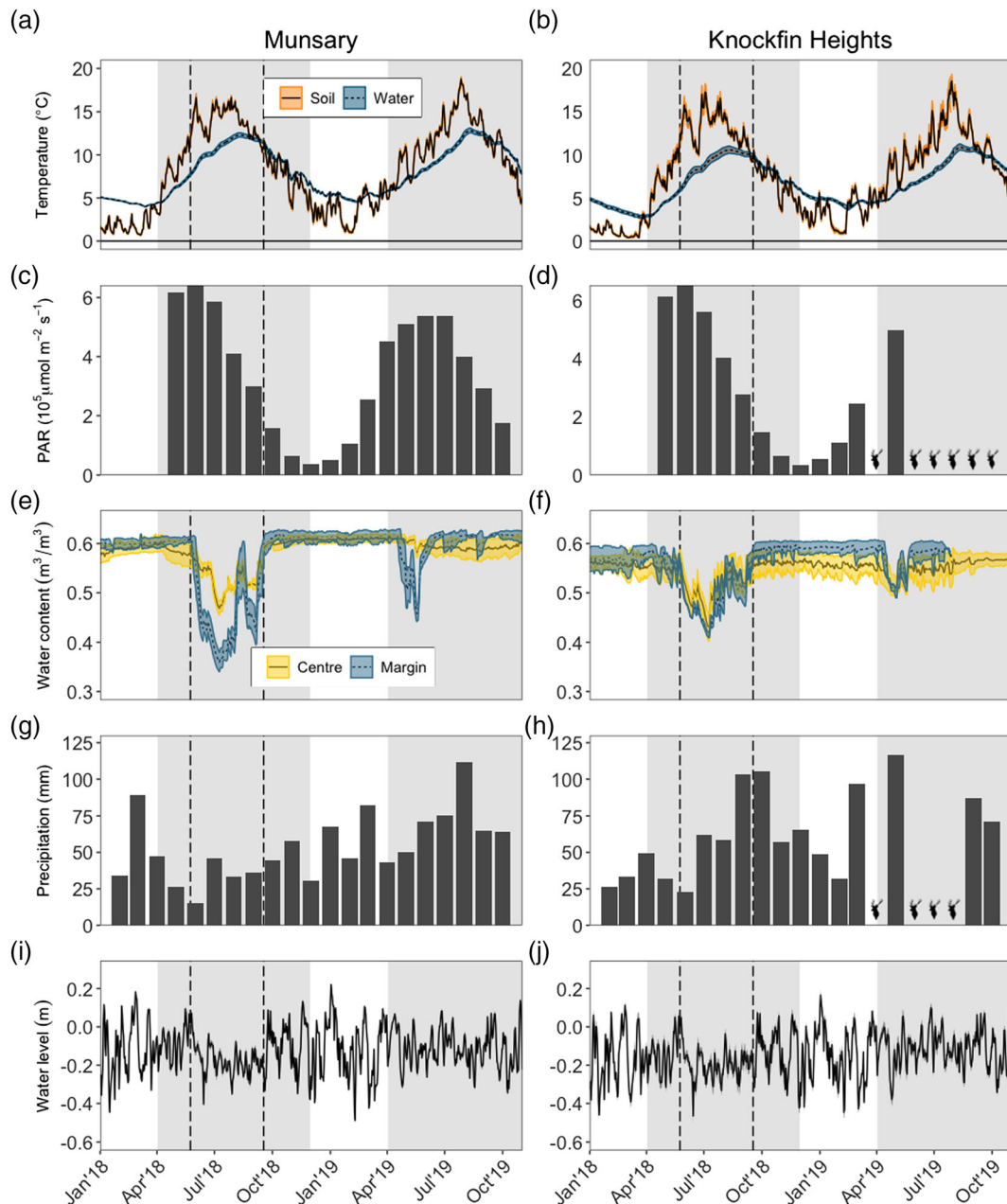


**FIGURE 3** Environmental data overview for Munsary and Knockfin Heights: daily average ( $\pm$ SE) of soil and water temperature (a,b); monthly cumulative photosynthetic active radiation (PAR) (c,d), daily average ( $\pm$ SE) soil water content for centre and margin plots (e,f), monthly cumulative precipitation (g,h) and daily average water level (i,j). Drought period (24 May 2018–17 September 2018) is indicated with dotted lines and growing season highlighted in grey (April–November). Missing values on Knockfin Heights when dataloggers were disabled by deer damage (d,h) are indicated with deer symbols.



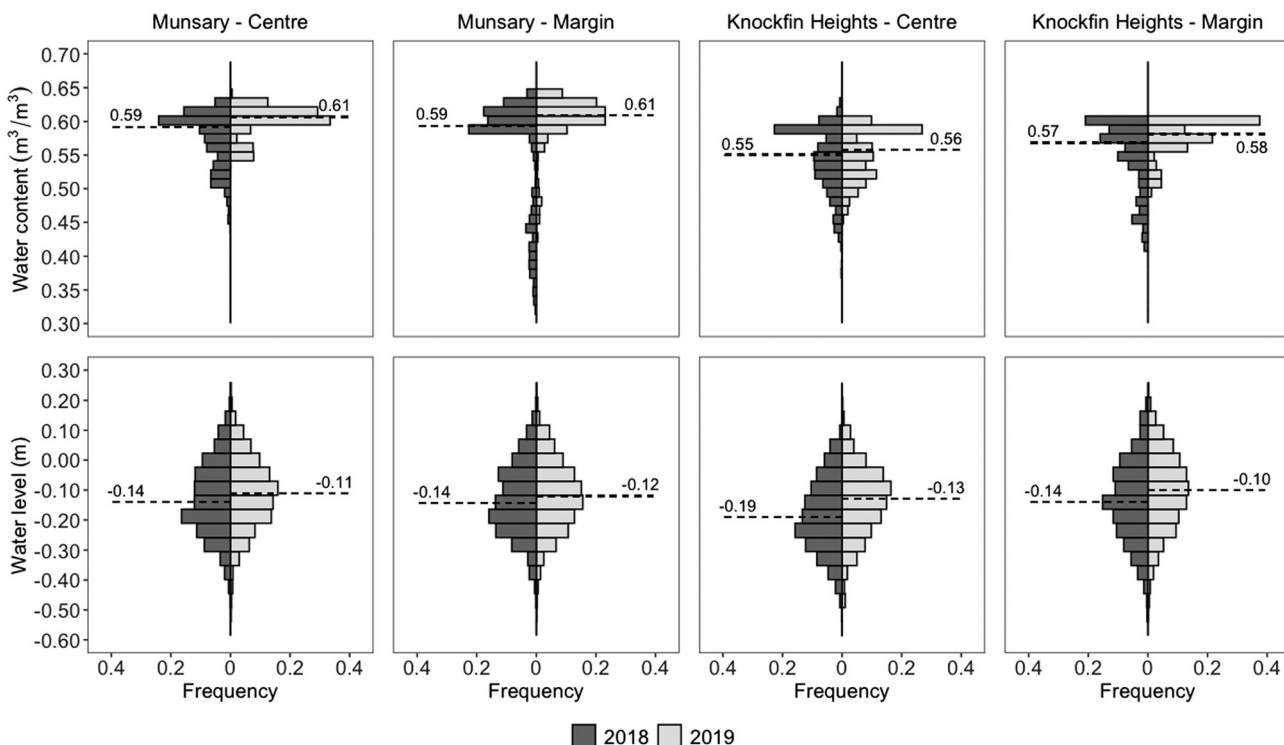


**FIGURE 4** Frequency distribution and median values of water content and water level for April–November in 2018 and 2019 for Munsary (low-lying) and Knockfin Heights (upland) centre and margin sites

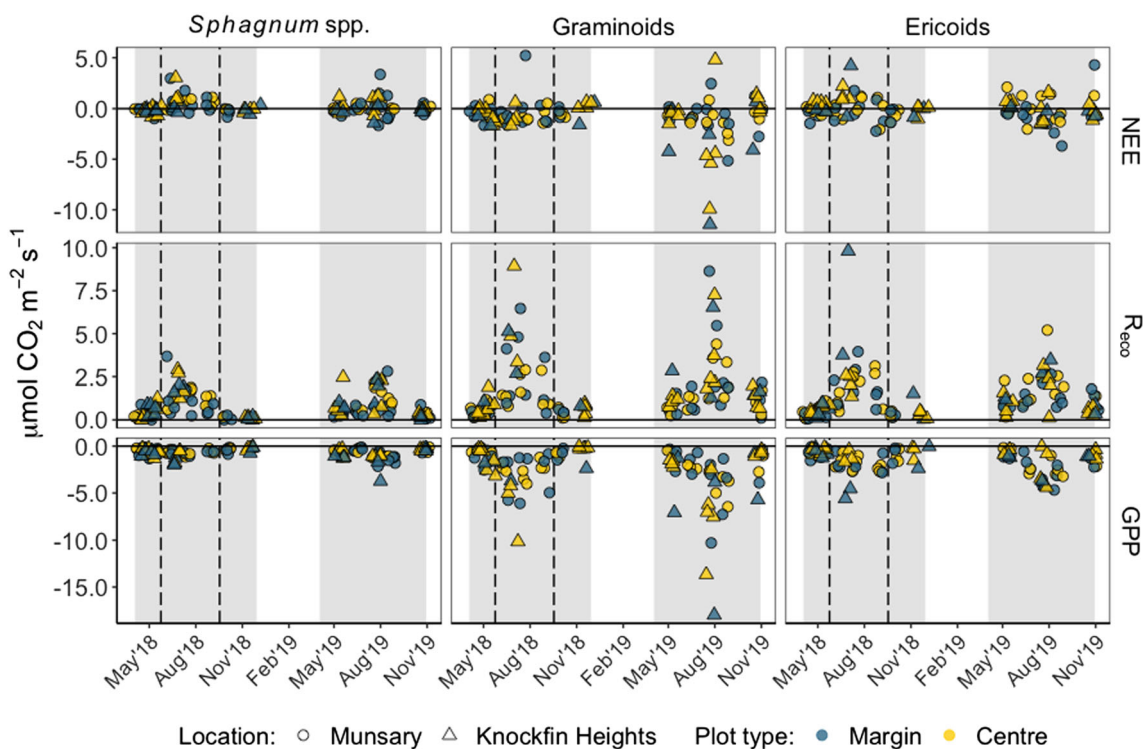


**FIGURE 5** Net ecosystem exchange (NEE), ecosystem respiration ( $R_{ecc}$ ) and gross primary production (GPP) fluxes for the three dominant plant functional types (PFTs) (*Sphagnum* spp., graminoids and ericoids) measured in 2018 and 2019. Drought period (24 May 2018–17 September 2018) is indicated with dotted lines and growing season highlighted in grey (April–November).

experienced higher soil water contents (medians between 0.59 and 0.61 m<sup>3</sup>/m<sup>3</sup>), compared to Knockfin Heights (median 0.55–0.58 m<sup>3</sup>/m<sup>3</sup>) (Figure 4). Microtopes also displayed variability (Figure 3e,f); margin sites had higher median soil water content, but more commonly experienced lower water content. Similarly, water level is skewed towards lower levels during the drier year 2018 (Figure 4): This decrease can be observed at both sites, with the largest differences for centre and margin plots at Knockfin Heights (Supporting information, Table S2). At both sites, water levels showed less variability during the drought period than during the spring, autumn and winter months (Figure 3i,j).

### 3.2 | In situ flux dynamics

A total of 1114 unique CO<sub>2</sub> flux measurements obtained from the blanket bog study sites and GPP flux rates were derived from the paired NEE and R<sub>eco</sub> flux estimates across the three dominant blanket bog PFTs (Figure 5) and other mosses, lichen, pools and bare peat (Supporting information, Figure S3).

There was no significant effect of study site and microtope on the variance across the fluxes for all PFTs and ground cover types ( $F(7,42.72) = 2.29, p = 0.13$ ). Only sampling year and PFT/ground cover type ( $F(7,471.18) = 2.66, p = 0.01$ ) were used for comparing inter-annual marginal means of the chamber measurements. No significant difference in mean interannual flux was observed between 2018 and 2019 from differing PFTs and key blanket bog features, with the exception of graminoid GPP (Figure 6). For 2018/2019, only in situ graminoid measurements reflect a net carbon sink (overall negative NEE) with ericoids being a sink in 2019, and other PFTs and ground cover types net sources of CO<sub>2</sub> (overall positive NEE). Mean NEE for *P. schreberi* and *C. uncialis/impexa* increased in 2019 compared to 2018, due to lower overall GPP and a slight increase in R<sub>eco</sub>; however, these differences were not significant ( $p > 0.05$ ). Increased respiration in 2019 can be observed in all categories, except for bare peat plots and pool measurements. For the bare peat and inundated bare peat collars, vegetation coverage (*E. angustifolium*)–*S. cuspidatum* for the pools—remained below 5%. Further, no more than 5% of the area in the *Sphagnum* spp. collars was affected by bleaching during the summer months at both study sites.

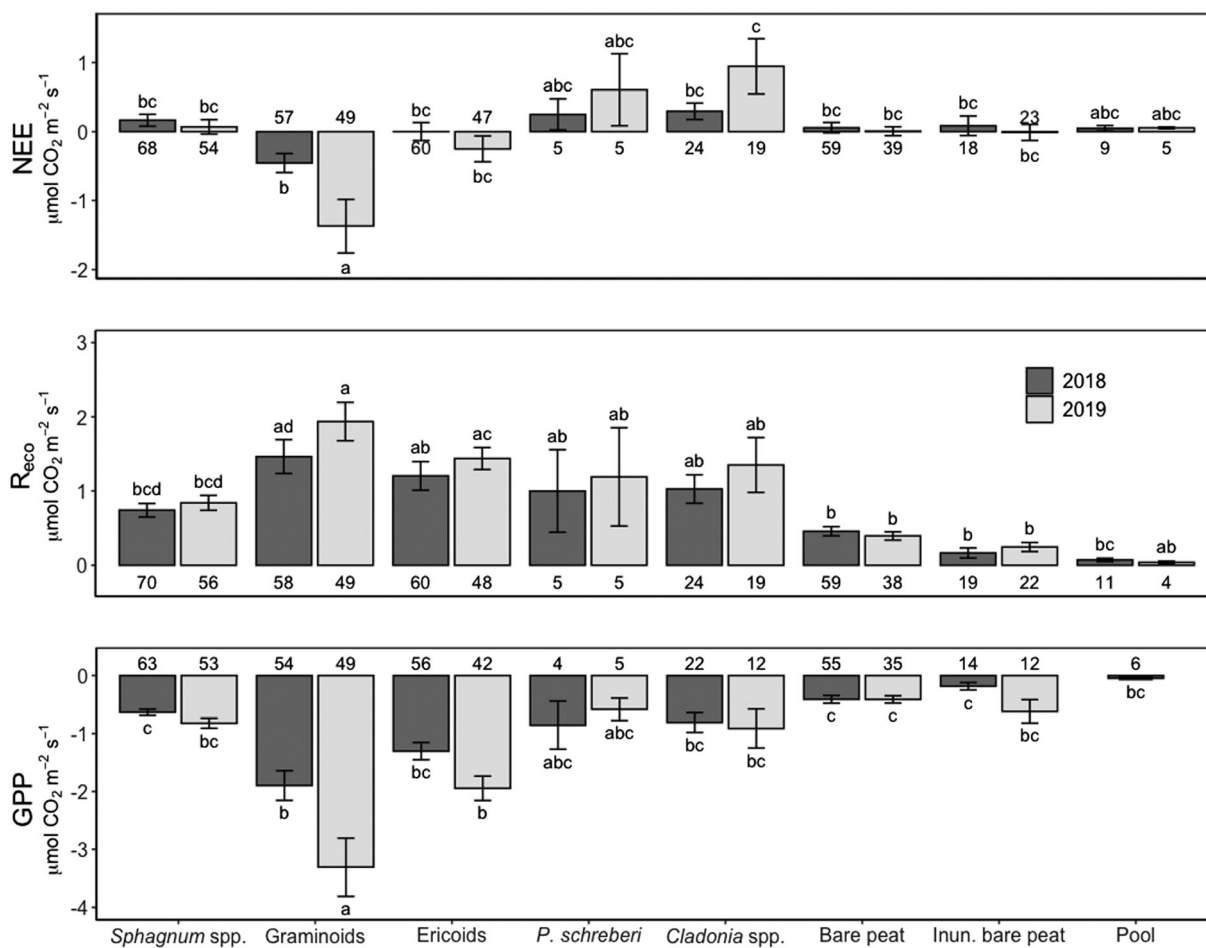


**FIGURE 6** Inter-annual mean ( $\pm$ SE) for all CO<sub>2</sub> fluxes from both sites, as: net ecosystem exchange (NEE); ecosystem respiration (R<sub>eco</sub>); and gross primary production (GPP) for both years across the plant functional types (PFTs) and ground cover types. Amongst flux types, shared letters are used for groups not significantly different ( $p > 0.05$ ), number represents sample size.

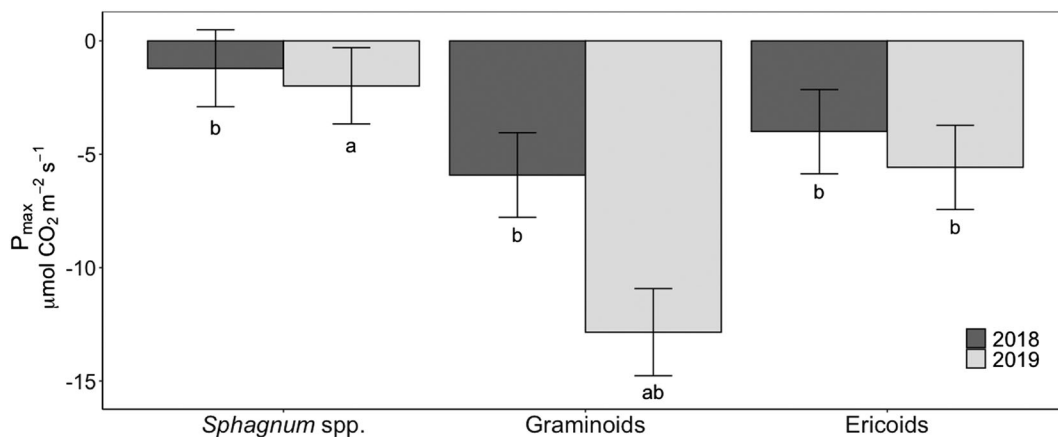


**FIGURE 7** Mean estimated potential maximum photosynthesis ( $P_{max}$ )  $\pm$  SE for the three dominant plant functional types (PFTs) (*Sphagnum* spp., graminoids and ericoids) for both years. Shared letters indicate no significant differences ( $p > 0.05$ ) between and across PFTs and years (Tukey post-hoc test).

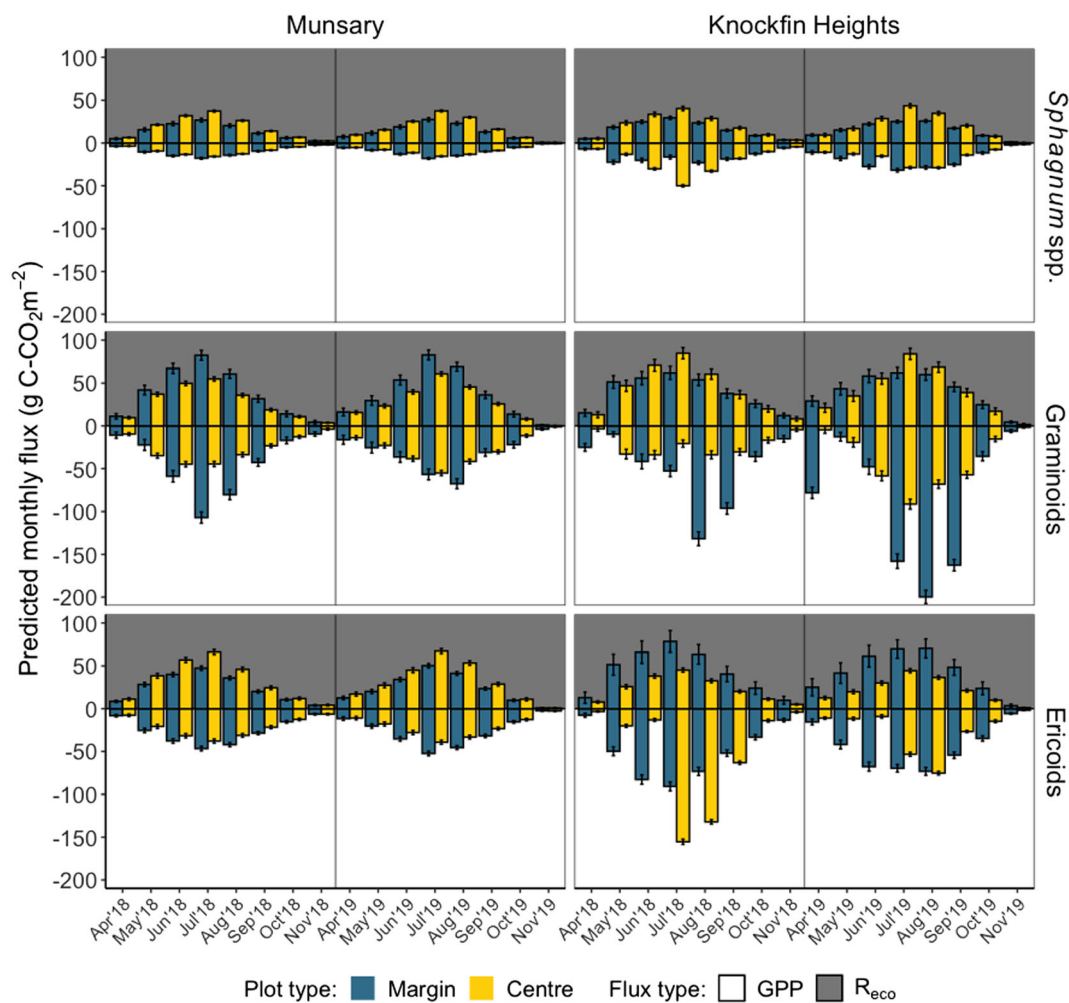


**FIGURE 8** Cumulative monthly modelled gross primary production (GPP) (negative range in white) and ecosystem respiration ( $R_{eco}$ ) (positive range in grey) for each plant functional type (PFT) at both sites across 2018 and 2019. Values show average cumulative flux ( $\text{g C-CO}_2 \text{ m}^{-2}$ ) with error bars to show range of cumulative fluxes across margin (blue) and centre (yellow) microtopes.

Comparisons of  $P_{\max}$  ( $\mu\text{mol CO}_2 \text{ m}^{-2} \text{ s}^{-1}$ ) of dominant PFTs show graminoids to have a significantly higher uptake value ( $-12.84 \pm 1.93$ ,  $n = 4$ ) in 2019 compared to the drought year 2018 ( $-5.91 \pm 1.87$ ,  $n = 5$ ) (Figure 7). Variability amongst *Sphagnum* spp.  $P_{\max}$  estimates was high (2018:  $-1.20 \pm 1.70$ ,  $n = 7$ ; 2019:  $-1.98 \pm 1.68$ ,  $n = 8$ ), contrasting with graminoid and ericoid predictions (2018:  $-3.99 \pm 1.86$ ,  $n = 5$ ; 2019:  $-5.57 \pm 1.86$ ,  $n = 5$ ) for both years. Significant effects were found when comparing  $P_{\max}$  means of the different PFTs (Figure 7, ( $F(2, 17.813) = 5.133$ ,  $p = 0.017$ ), year ( $F(1, 9.137) = 28.014$ ,  $p < 0.001$ ) and combined effect ( $F(2, 9.015) = 9.548$ ,  $p = 0.006$ )).

### 3.3 | Growing season GPP and $R_{\text{eco}}$

The predicted GPP and  $R_{\text{eco}}$  values showed strong linear correlations with the measured  $\text{CO}_2$  fluxes (Supporting information, Figures S4) for each of the PFT-site-microtope models (model parameters in Supporting information, Tables S4 and S5). For GPP,  $R^2$  values ranged between 0.43 and 0.91, with an overall  $\bar{x}_{rsq}$  of 0.80. GPP model RSE's were consistently lower for the centre fluxes compared to the margins. For  $R_{\text{eco}}$ , the  $R^2$  are lower than for GPP, ranging between 0.23 and 0.80, with an  $\bar{x}_{rsq} = 0.55$ .

The converted hourly GPP and  $R_{\text{eco}}$  estimates for each of the six blanket bog PFT-site-microtope combinations were summed to provide monthly estimates, highlighting variability across sites and PFTs during the sampling months (April–November 2018 and 2019) (Figure 8). The seasonal trend of increased respiration and productivity during the summer months is evident across all PFT-site-microtope variations. Monthly estimates from Knockfin Heights (April, May and November 2018/2019) of *Sphagnum* spp. GPP are similar to those of graminoids and ericoids in years. Highest predicted monthly GPP is seen amongst ericoids in 2018 (July:  $-155.4 \pm 3.1 \text{ g C-CO}_2 \text{ m}^{-2}$ ) and the graminoids in 2019 (August:  $-199.8 \pm 7.8 \text{ g C-CO}_2 \text{ m}^{-2}$ ). This disparity is not present in  $R_{\text{eco}}$  where both vascular plant types have similarly high monthly emissions compared to *Sphagnum* spp. estimates.

### 3.4 | Microtope variation of upland and low-lying blanket bog NEE

Cumulative NEE estimates for PFT-site-microtope combinates show the distribution of C- $\text{CO}_2$  fluxes for the growing season in both years is much more variable amongst the PFTs and microtopes across Knockfin Heights than at Munsary (Figure 9). Minimum and maximum

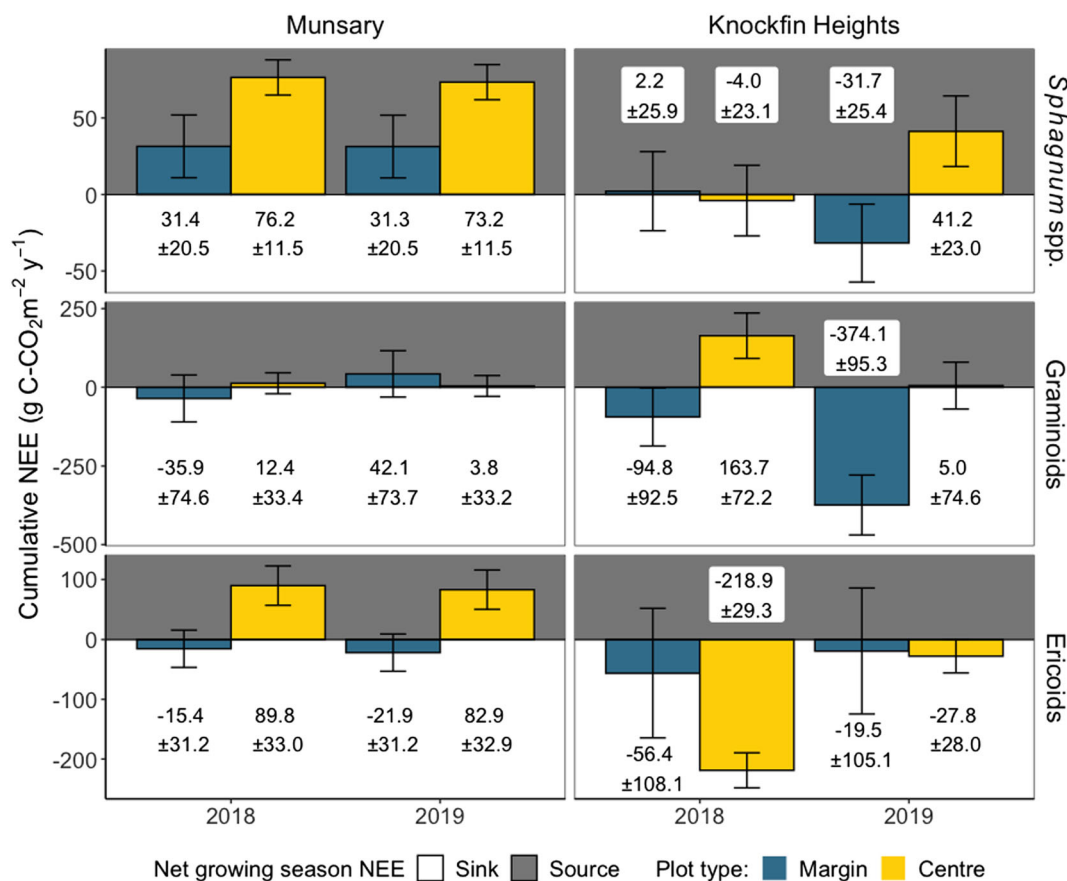


**FIGURE 9** Cumulative C- $\text{CO}_2$  net ecosystem exchange (NEE) balance ( $\pm$ range between maximum and minimum NEE from ecosystem respiration [ $R_{\text{eco}}$ ] and gross primary production [GPP] estimates) from for each dominant plant functional type (PFT) across both sites and blanket bog margin and centre microtopes across 2018 and 2019 (April 1st–November 31st)

**TABLE 1** Ranges in cumulative predicted net ecosystem exchange (NEE) across each site for both the drought (2018) and post-drought (2019) years using the maximum and minimum NEE (Figure 9). Change in ranges quantified as percentage increase or decrease in 2019 compared to the NEE ranges in 2018

	Munsary			Knockfin Heights		
	2018	2019	Change	2018	2019	Change
<i>Sphagnum</i> spp.	76.8	73.8	-3.9%	55.2	121.3	119.8%
Graminoids	156.3	147.4	-5.7%	233.6	549.0	135.0%
Ericoids	169.4	168.9	-0.3%	299.9	210.2	-29.9%

**TABLE 2** Parameter estimates for the fixed effects in the linear mixed-effects models of NEE,  $R_{eco}$  and GPP per plant functional type (PFT) and ground cover type

NEE	$R_{eco}$			GPP							
<i>Sphagnum</i> spp.											
$r^2 = 0.31$ , AIC = 143.39	$r^2 = 0.59$ , AIC = 145.30			$r^2 = 0.65$ , AIC = 91.78							
Estimate	SE	t	Estimate	SE	t	Estimate	SE	t			
Intercept	-0.13	0.09	-1.39	Intercept	0.75	0.14	5.30*	Intercept	-0.67	0.20	-3.35
Temp <sub>logger</sub>	0.19	0.06	3.12**	Temp <sub>logger</sub>	0.45	0.06	7.08**	Temperature	-0.29	0.04	-7.19**
Wcontent <sub>mean</sub>	-0.16	0.06	-2.87**	Wcontent <sub>mean</sub>	-0.19	0.06	-3.30**	Wcontent <sub>range</sub>	-0.11	0.04	-2.93**
Type: Centre	0.36	0.11	3.34**	Year: 2019	0.19	0.12	1.72	Year: 2019	-0.25	0.13	-1.89
Year: 2019	-0.02	0.12	-0.17								
Graminoids											
$r^2 = 0.32$ , AIC = 260.42	$r^2 = 0.65$ , AIC = 290.32			$r^2 = 0.96$ , AIC = 304.93							
Estimate	SE	t	Estimate	SE	t	Estimate	SE	t			
Intercept	-0.45	0.21	-2.12*	Intercept	1.58	0.51	3.11	Intercept	-2.34	4.99	-0.47
PAR	-0.27	0.11	-2.37*	Temperature	1.09	0.15	7.05**	Temperature	-1.58	0.15	-10.68**
Year: 2019	-0.52	0.22	-2.36*	Wcontent	-0.31	0.15	-2.04*	Wlevel <sub>mean</sub>	-0.47	0.14	-3.30**
				Year: 2019	0.54	0.27	1.98	Year: 2019	-0.66	6.99	-0.10
Ericoids											
$r^2 = 0.40$ , AIC = 232.76	$r^2 = 0.59$ , AIC = 256.15			$r^2 = 0.52$ , AIC = 228.75							
Estimate	SE	t	Estimate	SE	t	Estimate	SE	t			
Intercept	0.12	0.24	0.49	Intercept	1.30	0.41	3.20	Intercept	-1.34	0.29	-4.71*
PAR	-0.29	0.11	-2.71**	Temperature	0.82	0.16	5.19**	Temperature	-0.90	0.12	-7.42**
Trange <sub>logger</sub>	0.59	0.14	4.25**	Wcontent <sub>mean</sub>	-0.40	0.14	-2.94**	PAR	-0.23	0.11	-2.13*
Year: 2019	-0.42	0.26	-1.63	Year: 2019	0.69	0.29	2.39*	Trange <sub>logger</sub>	0.40	0.12	3.30**
								Year: 2019	-0.71	0.34	-2.10*

Abbreviations: AIC, Akaike information criterion; GPP, gross primary production; NEE, net ecosystem exchange; PAR, empirical in situ PAR measurements;  $R_{eco}$ , ecosystem respiration; Temperature, empirical in situ soil temperature measurements; Trange<sub>logger</sub>, daily soil temperature range (loggers); Wcontent, empirical in situ water content measurements; Wcontent<sub>mean</sub>, daily water content average (loggers); Wcontent<sub>range</sub>, daily water content range (loggers); Wlevel<sub>mean</sub>, daily water content average (loggers).

\* $p < 0.05$  (significance level for the covariate).

\*\* $p < 0.01$  (significance level for the covariate).

cumulative NEE ranges across Munsary were similar for all three PFTs between 2018 and 2019. At Knockfin Heights, flux estimate ranges doubled in the post-drought year for *Sphagnum* spp. and graminoids and were lower for ericoids (Table 1).

The increased range in NEE estimates on Knockfin Heights for graminoids is the result of higher predicted maximum net uptake of CO<sub>2</sub> in 2019 compared to the year before on the margin and centre plots (Figure 9). Similarly, at Munsary centre plots, predicted annual net CO<sub>2</sub> flux for graminoids was lower in 2019 but the margin

estimates show an opposite trend with an increase in net CO<sub>2</sub> emissions in 2019. This decrease in CO<sub>2</sub> sequestration is also observed in ericoid NEE estimates, but only on Knockfin Heights. However, both margin and centre plots are still likely to be net C-CO<sub>2</sub> sinks.

Switches between overall source and sink behaviour are observed on Knockfin Heights, where *Sphagnum* spp. on the margin plots moved towards a stronger C-CO<sub>2</sub> sink, but at the centre plots, the opposite occurred, with higher emission in 2019. Consistent CO<sub>2</sub> sources for both years are found in the *Sphagnum* spp. NEE estimates for Munsary,

with almost no changes between both years across margin and centre plots. Conversely, in the ericoids at Munsary, centre plots acted as sources and margin plots net sinks for both years (Figure 9).

### 3.5 | Environmental controls on in situ fluxes

GPP,  $R_{\text{eco}}$  and NEE fluxes in this study were driven by environmental conditions, and this relationship differed between the PFTs. The best performing models with Year included as a fixed effect had a soil temperature component to explain  $\text{CO}_2$  exchange variability (Table 2). Fluxes in the models are generally related to increases in soil

temperature, or daily soil temperature range in the case for ericoid NEE (pseudo  $r^2 = 0.40$ ) and GPP (pseudo  $r^2 = 0.52$ ). Only the graminoid NEE model did not include a temperature component, but rather a single PAR covariate to account for variability in net  $\text{CO}_2$  exchange (pseudo  $r^2 = 0.32$ ). The daily mean and range in peat water content also accounted for variance amongst flux estimates for *Sphagnum* spp. ( $R_{\text{eco}}$  pseudo  $r^2 = 0.59$ ; GPP pseudo  $r^2 = 0.65$ ), with similar, but stronger effects on  $R_{\text{eco}}$  fluxes for graminoids (pseudo  $r^2 = 0.65$ ) and ericoids (pseudo  $r^2 = 0.59$ ). Changes in daily mean water level accounted for graminoid GPP variance, with increasing uptake of  $\text{CO}_2$  associated with higher water levels. However, variation was still predominantly controlled by soil temperature (pseudo  $r^2 = 0.96$ ). As a

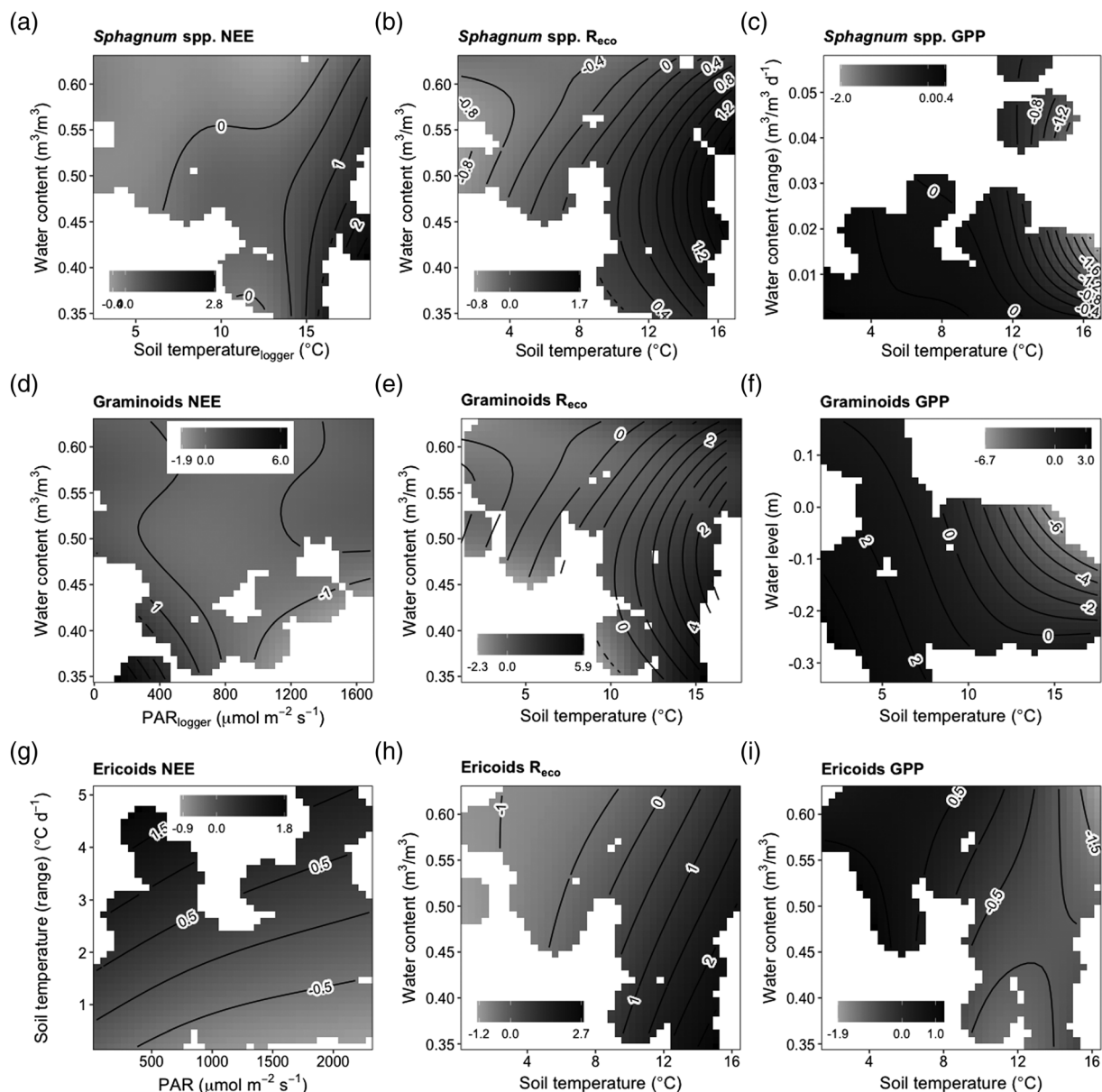


**FIGURE 10** Interactive fitted effects of environmental covariates on net ecosystem exchange (NEE), ecosystem respiration ( $R_{\text{eco}}$ ) and gross primary production (GPP) for *Sphagnum* spp. (a, b, c), graminoids (d, e, f) and ericoids (g, h, i). Only fitted flux values within the range of in situ environmental measurements are shown. Covariates include photosynthetic active radiation (PAR) (in situ or loggers), soil temperature (in situ or daily range from loggers), water content (daily mean or range from loggers) and water level (daily average).

fixed effect, *Year* was only a significant predictor of graminoid NEE and ericoid  $R_{\text{eco}}$  and GPP fluxes but was kept in all other models to account for variability across both sampling campaigns. Interactions between fixed effects did not improve model predictions with microtope type only applied to the *Sphagnum* spp. NEE model, where centre plots appear to be a more important predictor than *Year* for the period of sampling (pseudo  $r^2 = 0.31$ ).

### 3.6 | Non-linear effects

The GAMMs for the three dominant PFTs (*Sphagnum* spp., graminoids and ericoids) show non-linear interactive behaviour on modelled flux estimates for NEE,  $R_{\text{eco}}$  and GPP. The dominant covariates used in the models are soil temperature, mean and range of water content, PAR and mean water table depth (Figure 10). Since NEE fluxes are the product of  $R_{\text{eco}}$  and GPP, net flux dynamics of the different PFTs can be best explained by examining emission and sequestration processes separately.

$R_{\text{eco}}$  increased with higher soil temperatures ( $>10^\circ\text{C}$ ) and an optimum daily mean water content between  $0.4\text{--}0.6\text{ m}^3/\text{m}^3$  for *Sphagnum* spp. (Figure 10b) and  $0.35\text{--}0.55\text{ m}^3/\text{m}^3$  for graminoids (Figure 10e). An optimal moisture regime is not clear in ericoids  $R_{\text{eco}}$  but trends towards higher fluxes with drier soil conditions (Figure 10h). These relationships between temperature and water availability are replicated by GPP; however, the effect of drier conditions is more pronounced. GPP rates for *Sphagnum* spp. generally increase with soil temperature (above  $12^\circ\text{C}$ ) when daily fluctuations in water content are above  $0.04\text{ m}^3/\text{m}^3\text{ d}^{-1}$  (limited to days of high soil temperature and low daily precipitation) (Figure 10c). Graminoid GPP was highest during days with shallow water levels ( $<-0.15\text{ cm}$ ) and high soil temperatures ( $>12^\circ\text{C}$ ) (Figure 10f). However, these rates are restricted to the warmer seasons, during which almost no inundation occurred (daily soil temperature  $>11^\circ\text{C}$ ). Ericoid GPP was less well defined by the best model's covariates, soil temperature and average water content, showing an 'activity' threshold at soil temperatures of circa  $10^\circ\text{C}$ . Predicted fluxes are in the same range as *Sphagnum* spp. but show a much more gradual, less pronounced increase across both axes (Figure 10i).

The modelled NEE fluxes explain  $\text{CO}_2$  source and sink dynamics for the dominant PFTs. Fitted *Sphagnum* spp. NEE shows a gradual transition from sink (on days with soil water content values above  $0.45\text{ m}^3/\text{m}^3$  and soil temperatures between  $6$  and  $15^\circ\text{C}$ ) to source of  $\text{CO}_2$  when water availability decreases, and temperatures increase (Figure 10a). This behaviour changes to a rapid increase in emission rates for *Sphagnum* spp. above  $15^\circ\text{C}$ . Graminoids show similar transitions in NEE, with the addition of average daily PAR and average daily soil water content in the best performing GAMM. Most modelled graminoid NEEs show them to be an overall sink, although at PAR below  $600\text{ }\mu\text{mol m}^{-2}\text{ s}^{-1}$ , and soil water content values below  $0.45\text{ m}^3/\text{m}^3$  increased emissions, shifted them from a sink to a source of  $\text{CO}_2$  (Figure 10d). Similarly, the impact of changes in PAR on NEE can be observed for the ericoids, where lower radiation values together with

high daily changes in soil temperature ( $\pm 2^\circ\text{C d}^{-1}$ ) cause a shift towards higher emissions (Figure 10g). Net  $\text{CO}_2$  uptake for ericoids is restricted to days with low soil temperature variability across a range of PAR values. Modelled ericoid NEE shows a sink across high and low PAR values, similar to the average NEE of ericoids across both years (Figure 9), estimated across the measured PAR range at both sites.

## 4 | DISCUSSION

### 4.1 | Blanket bog PFTs $\text{CO}_2$ -fluxes

The 2018 drought was unforeseen, and consequently, this study was opportunistic, much like other studies in Europe (Hari et al., 2020; Saunders et al., 2021). The timing of events and the start of this study meant that there are no pre-drought summer fluxes making pre- and post-drought comparison impossible at these sites. Nonetheless, the two-year flux dataset reflects short-term  $\text{CO}_2$  dynamics (Sottocornola & Kiely, 2005; Strack et al., 2016) and provides meaningful insights when upscaled and observation uncertainty is accounted for (Gažovič et al., 2013).

There was no difference in variance between the NEE,  $R_{\text{eco}}$  and GPP fluxes for any PFTs or ground cover types between the drought and post-drought year, except for graminoid GPP and NEE (i.e., higher  $\text{CO}_2$  sequestration in 2019). However, estimated annual C- $\text{CO}_2$  flux estimates for the dominant vegetation groups do differ between the years, sites and microtopes and are likely controlled by the timing, severity and duration of the drought (Kross et al., 2014). All PFTs and key blanket bog features were likely strong net  $\text{CO}_2$  sources in both 2018 and 2019, apart from the ericoids in 2018 and graminoids in 2019 (microtope centres, Knockfin Heights), which were strong net  $\text{CO}_2$  sinks. Similar net  $\text{CO}_2$  source behaviour amongst the same peatland PFTs was also observed in Irish peatland for the same years (2018–19) (Saunders et al., 2021) and Sweden on an ombrotrophic blanket bog (Keane et al., 2020), although emissions recovered in 2019 to pre-drought rates. Though not measured in this study, higher temperatures likely also contributed to increased microbial respiration (Järveoja et al., 2020; Keiser et al., 2019).

For non-vegetated sites (bare peat collars), the steady overall net  $\text{CO}_2$  emissions measured were in line with other sites in the UK (Clay et al., 2012; Dixon et al., 2014; Gatis et al., 2019). The slight increase in  $\text{CO}_2$  emissions observed in inundated bare peat collars and floating chamber measurements in 2019 could reflect increased mineralisation associated with biogeochemical and microbial cascades associated with the 'enzymic latch' observed in peatlands following drought-rewetting cycles (Fenner & Freeman, 2011). In pools at Munsary, increased mineralisation rates have been associated with high DOC concentrations and correlated with higher dissolved  $\text{CO}_2$  concentrations (Turner et al., 2016) and net  $\text{CO}_2$  emissions. For vegetated sites, earlier onset of growing season (associated with higher spring temperatures) is not expected to influence cumulative GPP for northern peatlands (Kross et al., 2014). However, it can negatively affect annual

NEE, when short, severe drought periods in peak growing season increase  $R_{\text{eco}}$ , but not GPP (Lund et al., 2012). This is observed for *Sphagnum* spp., ericoids and graminoids across both sites, where  $R_{\text{eco}}$  estimates are higher in Spring of 2018, compared to Spring 2019 when conditions were wetter.

Previous studies have found that drought effect is strengthened by topographical setting, with *Sphagnum* species at higher topographic elevations suffering from a stronger negative effect on net  $\text{CO}_2$  exchange during periods of increased temperature (Gerdol & Vicentini, 2011). Recovery to pre-drought conditions is possible when drought conditions do not cross lethal thresholds (prolonged extreme high temperatures and low precipitation), or when *Sphagnum* bleaching is minimal. *Sphagnum* hummocks in Italian upland bogs (>1000 m. a.s.l.) showed signs of irreversible desiccation during a heatwave in 2003, but recovery of *Sphagnum* species in hollows and lawns was reported in the following year (Bragazza, 2008). However, this study shows the opposite trend, with higher modelled productivity during the 2018 drought for *Sphagnum* spp. at the higher elevations of Knockfin Heights compared to Munsary ( $\pm 250$  m difference). Despite a consistent negative precipitation anomaly for the low-lying and upland site compared to the long-term average across Northern Scotland (Supporting information, Figure S2), Knockfin Heights experienced a smaller anomaly towards the end of the sampling period, mitigating some of the early drought impact from the dry spring months. This difference is in line with the east–west gradient of increasing rainfall across the Flow Country region (Lindsay et al., 1988). Importantly, blanket bogs rely on occult precipitation, which can contribute up to 20% of their water input (Lapen et al., 2000). It is therefore possible that at 350 m above sea level, Knockfin Heights experienced more frequent fog and increased dew-fall, effectively reducing the site water deficit and avoiding *Sphagnum* spp. ‘shut down’.

The drought of 2018 led to surface subsidence at both Munsary and Knockfin Heights of between 5–10 and 1–2 cm, respectively (Marshall et al., 2019; Marshall et al., 2022). Lowering of the surface following water level drops in the peat is predicted to mitigate against drought conditions by allowing higher water content to be sustained at the peat surface (Price, 2003) and increasing water availability for the blanket bog vegetation (Lapen et al., 2000). Peat surface subsidence and its potential to buffer against water level drawdown could explain why some of the PFTs were still overall  $\text{CO}_2$  sinks during the 2018 period, as water deficits may not have reached critical thresholds, (e.g., graminoids at margin plots on Knockfin Heights [Figure 9]).

Since water level is used for the modelled cumulative GPP and  $R_{\text{eco}}$  estimates, high subsidence rates at Munsary resulting in the peatland surface effectively tracking the water table could explain similar annual estimates for both drought and post-drought years. For Munsary, this explains NEE estimates for all but the graminoids in the margin plots, where annual estimates switch to net  $\text{CO}_2$  sources. Although Knockfin Heights experienced more variable water levels and marginally drier conditions, Munsary margin plots experienced more frequent and prolonged lower soil water contents during 2018 (Figures 3 and 4). This supports the observation that blanket bog

margins show higher  $\text{CO}_2$  flux due to higher environmental variability (i.e., water level and subsidence rates) in response to drought. It is possible that graminoids in margin areas at Munsary, identified as areas of high subsidence rates (Alshammari et al., 2018; Marshall et al., 2019; Marshall et al., 2022), could be responding (lower GPP, higher  $R_{\text{eco}}$ ) to structural alterations of the peat surface (i.e., cracks and bare peat exposure) in the post-drought year.

## 4.2 | Relating drought effects on $\text{CO}_2$ fluxes to environmental conditions

Drought effects on fluxes across the PFTs can be summarised by the effects of increased soil temperatures and changes in water availability. Ericoids showed a stronger increase in both  $\text{CO}_2$  sequestration and respiration rates (GPP and  $R_{\text{eco}}$ ) compared to *Sphagnum* spp. and graminoids in the post-drought year. Acknowledged is that the increased  $R_{\text{eco}}$  fluxes could also be explained by increased methane oxidation during drier upper peat condition (Freeman et al., 2002), though this was outside the scope of this study. The resilience pattern of ericoids > graminoids > *Sphagnum* spp. compares well with results from other ombrotrophic bog studies (Bubier et al., 2003; Goud et al., 2017), due to the physiological advantage of vascular plants to better stabilise their  $\text{CO}_2$  fluxes during drier conditions by actively taking up water and limiting transpiration. Conversely, increased water availability promoted *Sphagnum* spp. GPP and graminoid GPP (dominated by *Eriophorum* spp.) in line with their preference for overall wet conditions in blanket bogs (Laine et al., 2007) and peatlands in general (Cooper et al., 2014; Van Breemen, 1995). Increased water availability and higher water levels also increase  $R_{\text{eco}}$ , something also observed in shallow peat cores from a site 10 km west of Knockfin Heights (Hermans et al., 2019) and a rewetting experiment on similar PFTs (Kuiper et al., 2014).

Accounting for different light intensities, drought conditions did not have a significant effect on the productivity estimates ( $P_{\text{max}}$ ) for *Sphagnum* spp. and ericoids. Uptake estimates in 2018 were lower for graminoids (Figure 7) with modelled maximum GAMM GPP compared to  $P_{\text{max}}$  estimates ( $-6.7$  against  $-12.8 \mu\text{mol CO}_2 \text{ m}^{-2} \text{ s}^{-1}$ ), indicating that the graminoids had not returned to optimal condition in 2019 and remained limited in their productivity (Strachan et al., 2016). Similarly, both measured and modelled ranges for *Sphagnum* spp. and ericoid GPP in 2019 remained below  $P_{\text{max}}$  estimates. The general lower light saturation point of bryophytes (Marschall & Proctor, 2004) and comparable PAR regimes across 2018 and 2019 (Figure 3c,d) could explain the consistency of maximum productivity estimates. The uniformity of in situ fluxes and  $P_{\text{max}}$  estimates suggests that conditions were not (yet) limiting *Sphagnum* spp. productivity, evidenced by the limited *Sphagnum* bleaching observed in the field. Overall, the response of *Sphagnum* spp. to reduce water levels was likely less severe than hypothesised, for example, a substantial reduction in productivity (Jassey & Signarbieux, 2019; Strack et al., 2009).

PAR was only a dominant driver for ericoid GPP, suggesting that ericoid photosynthetic activity was not limited by water availability. This highlights ericoid shrub drought resilience through their adaptive



traits to retain moisture and nutrients (Aerts, 1999; Bubier et al., 2003; Kool & Heijmans, 2009). Ericoids mostly act as a CO<sub>2</sub> sink, contributing to overall peatland NEE (Kuiper et al., 2014). However, Munsary centre plots (dominated by *C. vulgaris*) behaved as a positive net CO<sub>2</sub> source. NEE estimates for a range of *C. vulgaris* age/height ranges show that annual sinks are not common (Laine et al., 2007) with only the Munsary centre plots having comparable ericoid shrub age/height ranges. Since there is no evidence of recent management that could have influenced the natural ericoid shrub maturation at both sites, a potential bias towards plots with established ericoid cover could have excluded the less dominant, juvenile *C. vulgaris* that might have shifted the estimates closer to a net C-CO<sub>2</sub> sink.

### 4.3 | Mean annual water level (MAWL) and global peatland NEE estimates

Comparing growing season NEE C-CO<sub>2</sub> estimates of the dominant PFTs in this study with estimates from other peatland sites shows that overall the NEE estimates ( $-10.2 \pm 106.4$  g C-CO<sub>2</sub> m<sup>-2</sup> yr<sup>-1</sup>) are within range of other intact/near-natural blanket bogs ( $-75.4 \pm 48.0$  g C-CO<sub>2</sub> m<sup>-2</sup> yr<sup>-1</sup>), other bogs ( $-21.0 \pm 91.9$  g C-CO<sub>2</sub> m<sup>-2</sup> yr<sup>-1</sup>) and fens ( $-70.3 \pm 39.0$  g C-CO<sub>2</sub> m<sup>-2</sup> yr<sup>-1</sup>) (Figure 11). Most (blanket) bog NEE estimates are from EC measurements, with large footprints, whereas CO<sub>2</sub> estimates from chamber-based studies include micro-scale targets. Nonetheless, the multi-annual estimates from the studies involved allow for comparisons with MAWL variability in northern peatlands (Swenson et al., 2019).

MAWL for the upland and low-lying site (Supporting information, Table S2) is also comparable to that of intact/near-natural sites ( $-9.6 \pm 8.3$  cm), mostly staying above the MAWL of bare peat sites ( $-24.5 \pm 17.5$  cm) and drained/restored sites ( $-26.0 \pm 20.7$  cm). Net C-CO<sub>2</sub> sink and source behaviour related to MAWL is visible in the other peatland types where annual and seasonal NEE (g C-CO<sub>2</sub> m<sup>-2</sup> yr<sup>-1</sup>) estimates show a general increase in net emission with lower MAWL (Figure 9). Generally, lower water levels—in these cases linked to peatland type and restoration or management history—correspond with higher overall C-CO<sub>2</sub> emissions. This relationship was estimated to be strong for all vegetated sites and less so for the bare peat sites, being overall CO<sub>2</sub> sources (Swenson et al., 2019). However, MAWL between the drought and post-drought year only explains a minor part of the water deficit differences across the plots in this study, and water-stress estimates for PFTs are better reflected in observed soil water content relationships (GAMM results).

### 4.4 | Future blanket bog drought resilience

The CO<sub>2</sub> balance of the PFTs and key blanket bog features in this study shows that the Flow Country peatlands are sensitive to drought conditions (Fenner & Freeman, 2011; Lund et al., 2012). Changes in the long-term functional state (net sink vs. net source) of blanket bogs are expected to depend on the frequency and duration of predicted droughts in Scotland (Grillakis, 2019). Repeated droughts are likely to trigger a shift to more drought resilient vascular plant species and *Sphagnum* spp. replacing other species occupying similar ecological

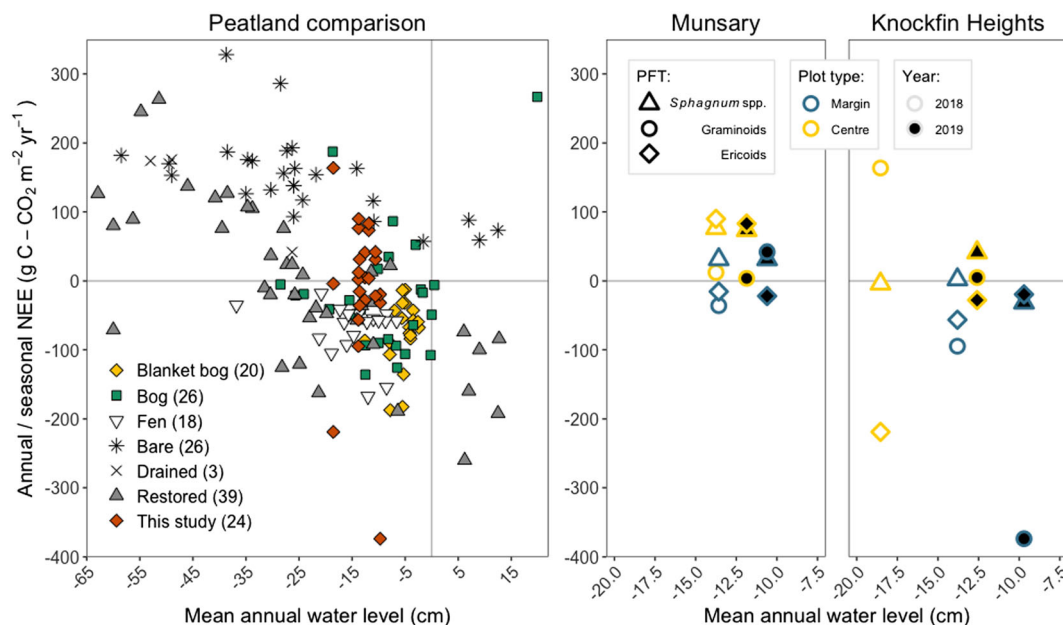


**FIGURE 11** Left: comparison of annual/seasonal net ecosystem exchange (NEE) estimates plotted against mean annual water level for global studies on boreal and temperate peatlands, including bare peat sites, (near-)natural blanket bogs, fens and other bogs, drained and restored sites (adapted from Swenson et al., 2019) and the modelled estimates from this study. Number in brackets in legend signifies data point count for each category in the plot. Right: seasonal NEE estimates for *Sphagnum* spp., graminoids and ericoids for both sites, across margin and centre plots for 2018 and 2019: C-CO<sub>2</sub> ranges are left out for simplicity, please refer to Figure 9.

niches, which are unable to adapt (Robroek et al., 2017). For example, shifts from *Sphagnum* spp. to more resilient bryophyte species during prolonged periods of droughts such as *Polytrichum* (Potvin et al., 2014) or *R. lanuginosum* (Lindsay, 2010) could also be expected.

Changing blanket bog vegetation composition during and after drought conditions (i.e., upland graminoids and ericoids) also results in higher biomass and litter load (Grau-Andrés et al., 2018), which alongside changing climate will make peatland more vulnerable to wildfires (Granath et al., 2016) and fire-related emissions. This coupled with drought-induced structural peat surface alterations—that is, cracks and drier conditions (Li et al., 2018)—also helps facilitate prolonged smouldering, increasing peat fire hazard (Davies et al., 2013). This risks creating positive feedback loops where drought and fire frequency increases at the cost of peatland resilience (Field et al., 2007), offsetting any gains in productivity.

Together with novel remote sensing techniques (Alshammari et al., 2018, 2020; Fiaschi et al., 2019; Marshall et al., 2022; Tampuu et al., 2020) and accurate land-cover estimates, the flux estimates from the margins and centre plots at the upland and low-lying site provide insight into the blanket bog response characteristics across a range of dominant vegetation types during and after an extreme drought. The ability to differentiate between PFT and key blanket bog features highlights the unique response each type is likely to have in response to a predicted shift towards drier and warmer summers and the impact on carbon fluxes on blanket bogs across the United Kingdom.

## 5 | CONCLUSION

Overall, our study shows that estimating CO<sub>2</sub> fluxes of PFTs and key blanket bog features is valuable to understand different responses during and after a drought event. With these growing season flux estimates, we were able to show a drought resilience pattern of ericoids > graminoids > *Sphagnum* spp. at both upland and low-lying sites. The relation to water availability and their topographic setting suggests that if drought frequency and severity increase, blanket bog vegetation is expected to shift towards assemblages that can cope with these conditions (i.e., ericoid shrubs). Since these hydrological conditions are expected to become more frequent, it is important to establish baseline studies to understand the long-term impact of these extreme events (e.g., drought and wildfires) on carbon fluxes. This will require upscaling using vegetation as a proxy for GHG emissions to assess landscape scale drought-responses, post-fire recovery studies or even national and global climate impact predictions and requires integration with remote sensing measurements, including the deployment of unoccupied aerial vehicles (UAVs) for increased detail and more long-term monitoring on peatlands to assess the effectiveness of conservation management.

## ACKNOWLEDGEMENTS

HPS was funded through a PhD project supported by the European Social Fund and Scottish Funding Council as part of Developing

Scotland's Workforce in the Scotland 2014–2020 European Structural and Investment Fund Program. RA and CM are funded through Natural Environment Research Council (NERC) grant NE/P014100/1. RA is supported by a Leverhulme Leadership Award RL2019-0002. Purchase of the PAR-sensors was made possible by the awarded Allan Robertson grant from the International Peatland Society in 2018. We are grateful to the RSPB Forsinard Flows, in particular Daniela Klein, and Plantlife Scotland for supporting us with field preparations. We also thank Jasmijn Sybenga, Natalie Isaksson and Julia Avercamp for helping in the field.

## DATA AVAILABILITY STATEMENT

The data that support the findings of this study are openly available in NERC Environmental Information Data Centre at <https://doi.org/10.5285/1be4eef2-0591-4073-bae2-e00b6ff4462f>.

## ORCID

Henk Pieter Sterk  <https://orcid.org/0000-0002-2421-7066>

Chris Marshall  <https://orcid.org/0000-0003-4941-2199>

## REFERENCES

- Aerts, R. (1999). Interspecific competition in natural plant communities: Mechanisms, trade-offs and plant-soil feedbacks. *Journal of Experimental Botany*, 50(330), 29–37. <https://doi.org/10.1093/jxb/50.330.29>
- Alshammari, L., Large, D. J., Boyd, D. S., Sowter, A., Andersen, R., Andersen, R., & Marsh, S. (2018). Long-term peatland condition assessment via surface motion monitoring using the ISBAS DInSAR technique over the Flow Country, Scotland. *Remote Sensing*, 10(7), 1103. <https://doi.org/10.3390/rs10071103>
- Alshammari, L., Boyd, D. S., Sowter, A., Marshall, C., Andersen, R., Gilbert, P., Marsh, S., & Large, D. J. (2020). Use of surface motion characteristics determined by InSAR to assess peatland condition. *Journal of Geophysical Research - Biogeosciences*, 125(1). <https://doi.org/10.1029/2018JG004953>
- Andersen, R., Cowie, N., Payne, R. J., & Subke, J. A. (2019). The Flow Country Peatlands of Scotland: Foreword. *Mires and Peat*, 23, 1–2.
- Armstrong, A., Waldron, S., Ostle, N. J., Richardson, H., & Whitaker, J. (2015). Biotic and abiotic factors interact to regulate northern peatland carbon cycling. *Ecosystems*, 18(8), 1395–1409. <https://doi.org/10.1007/s10021-015-9907-4>
- Avercamp, J., Marshall, C., Sterk, H.P., Gilbert, P., Andersen, R., Marsh, S., & Large, D.J. (2021). Peat characteristic data from Blanket Peatland in the Flow Country, Caithness and Sutherland, 2018; (dataset); NERC EDS Environmental Information Data Centre: Lancaster, UK. <https://doi.org/10.5285/3458e0b9-5002-4ddb-bcb3-1c7fb08fb70b>
- Bates, D., Mächler, M., Bolker, B. M., & Walker, S. C. (2015). Fitting linear mixed-effects models using lme4. *Journal of Statistical Software*, 67(1), 1–48. <https://doi.org/10.18637/jss.v067.i01>
- Bengtsson, F., Granath, G., & Rydin, H. (2016). Photosynthesis, growth, and decay traits in sphagnum – A multispecies comparison. *Ecology and Evolution*, 6(10), 3325–3341. <https://doi.org/10.1002/ece3.2119>
- Berg, A., & Sheffield, J. (2018). Soil moisture-evapotranspiration coupling in CMIP5 models: Relationship with simulated climate and projections. *Journal of Climate*, 31(12), 4865–4878. <https://doi.org/10.1175/JCLI-D-17-0757.1>
- Berger, S., Praetzel, L. S. E., Goebel, M., Blodau, C., & Knorr, K. H. (2018). Differential response of carbon cycling to long-term nutrient input and altered hydrological conditions in a continental Canadian peatland. *Biogeosciences*, 15(3), 885–903. <https://doi.org/10.5194/bg-15-885-2018>

- Bragazza, L. (2008). A climatic threshold triggers the die-off of peat mosses during an extreme heat wave. *Global Change Biology*, 14(11), 2688–2695. <https://doi.org/10.1111/j.1365-2486.2008.01699.x>
- Bubier, J. L., Bhatia, G., Moore, T. R., Roulet, N. T., & Lafleur, P. M. (2003). Spatial and temporal variability in growing-season net ecosystem carbon dioxide exchange at a large peatland in Ontario, Canada. *Ecosystems*, 6(4), 430–441. <https://doi.org/10.1007/s10021-003-0125-0>
- Buras, A., Rammig, A., & Zang, S. (2020). Quantifying impacts of the 2018 drought on European ecosystems in comparison to 2003. *Biogeosciences*, 17(6), 1655–1672. <https://doi.org/10.5194/bg-17-1655-2020>
- Burnham, K. P., & Anderson, D. R. (2004). Multimodel inference: Understanding AIC and BIC in model selection. *Sociological Methods & Research*, 33, 261–304. <https://doi.org/10.1177/0049124104268644>
- Chan, D., Cobb, A., Zeppetello, L. R. V., Battisti, D. S., & Huybers, P. (2020). Summertime temperature variability increases with local warming in midlatitude regions. *Geophysical Research Letters*, 47(13). <https://doi.org/10.1029/2020GL087624>
- Chan, S. C., Kahana, R., Kendon, E. J., & Fowler, H. J. (2018). Projected changes in extreme precipitation over Scotland and Northern England using a high-resolution regional climate model. *Climate Dynamics*, 51(9–10), 3559–3577. <https://doi.org/10.1007/s00382-018-4096-4>
- Chaudhary, N., Westermann, S., Lamba, S., Shurpali, N., Sannel, A. B. K., Schurgers, G., Miller, P. A., & Smith, B. (2020). Modelling past and future peatland carbon dynamics across the pan-Arctic. *Global Change Biology*, 26(7), 4119–4133. <https://doi.org/10.1111/gcb.15099>
- Clark, J. M., Gallego-Sala, A. V., Allott, T. E. H., Chapman, S. J., Farewell, T., Freeman, C., House, J. I., Orr, H. G., Prentice, I. C., & Smith, P. (2010). Assessing the vulnerability of blanket peat to climate change using an ensemble of statistical bioclimatic envelope models. *Climate Research*, 45(1), 131–150. <https://doi.org/10.3354/cr00929>
- Clay, G. D., Dixon, S., Evans, M. G., Rowson, J. G., & Worrall, F. (2012). Carbon dioxide fluxes and DOC concentrations of eroding blanket peat gullies. *Earth Surface Processes and Landforms*, 37(5), 562–571. <https://doi.org/10.1002/esp.3193>
- Cooper, M. D. A., Evans, C. D., Zielinski, P., Levy, P. E., Gray, A., Peacock, M., Norris, D., Fenner, N., & Freeman, C. (2014). Infilled ditches are hotspots of landscape methane flux following peatland rewetting. *Ecosystems*, 17(7), 1227–1241. <https://doi.org/10.1007/s10021-014-9791-3>
- Davies, G. M., Gray, A., Rein, G., & Legg, C. J. (2013). Peat consumption and carbon loss due to smouldering wildfire in a temperate peatland. *Forest Ecology and Management*, 308, 169–177. <https://doi.org/10.1016/j.foreco.2013.07.051>
- Dieleman, C. M., Branfireun, B. A., McLaughlin, J. W., & Lindo, Z. (2015). Climate change drives a shift in peatland ecosystem plant community: Implications for ecosystem function and stability. *Global Change Biology*, 21(1), 388–395. <https://doi.org/10.1111/gcb.12643>
- Dixon, S. D., Qassim, S. M., Rowson, J. G., Worrall, F., Evans, M. G., Boothroyd, I. M., & Bonn, A. (2014). Restoration effects on water table depths and CO<sub>2</sub> fluxes from climatically marginal blanket bog. *Biogeochemistry*, 118(1–3), 159–176. <https://doi.org/10.1007/s10533-013-9915-4>
- Dunn, C., Jones, T. G., Roberts, S., & Freeman, C. (2016). Plant species effects on the carbon storage capabilities of a blanket bog complex. *Wetlands*, 36(1), 47–58. <https://doi.org/10.1007/s13157-015-0714-7>
- Fasiolo, M., Nedellec, R., Goude, Y., & Wood, S. N. (2020). Scalable visualization methods for modern generalized additive models. *Journal of Computational and Graphical Statistics*, 29(1), 78–86. <https://doi.org/10.1080/10618600.2019.1629942>
- Fenner, N., & Freeman, C. (2011). Drought-induced carbon loss in peatlands. *Nature Geoscience*, 4(12), 895–900. <https://doi.org/10.1038/ngeo1323>
- Fiaschi, S., Holohan, E. P., Sheehy, M., & Floris, M. (2019). PS-InSAR analysis of Sentinel-1 data for detecting ground motion in temperate oceanic climate zones: A case study in the Republic of Ireland. *Remote Sensing*, 11(3), 348. <https://doi.org/10.3390/rs11030348>
- Field, C. B., Lobell, D. B., Peters, H. A., & Chiariello, N. R. (2007). Feedbacks of terrestrial ecosystems to climate change. *Annual Review of Environment and Resources*, 32, 1–29. <https://doi.org/10.1146/annurev.energy.32.053006.141119>
- Forzieri, G., Feyen, L., Rojas, R., Flörke, M., Wimmer, F., & Bianchi, A. (2014). Ensemble projections of future streamflow droughts in Europe. *Hydrology and Earth System Sciences*, 18(1), 85–108. <https://doi.org/10.5194/hess-18-85-2014>
- Freeman, C., Nevison, G. B., Kang, H., Hughes, S., Reynolds, B., & Hudson, J. A. (2002). Contrasted effects of simulated drought on the production and oxidation of methane in a mid-Wales wetland. *Soil Biology and Biochemistry*, 34(1), 61–67. [https://doi.org/10.1016/S0038-0717\(01\)00154-7](https://doi.org/10.1016/S0038-0717(01)00154-7)
- Gallego-Sala, A. V., & Colin Prentice, I. (2013). Blanket peat biome endangered by climate change. *Nature Climate Change*, 3(2), 152–155. <https://doi.org/10.1038/nclimate1672>
- Gallego-Sala, A. V., Clark, J. M., House, J. I., Orr, H. G., Prentice, I. C., Smith, P., Farewell, T., & Chapman, S. J. (2010). Bioclimatic envelope model of climate change impacts on blanket peatland distribution in Great Britain. *Climate Research*, 45(1), 151–162. <https://doi.org/10.3354/cr00911>
- Gatis, N., Benaud, P., Ashe, J., Luscombe, D. J., Grand-Clement, E., Hartley, I. P., Anderson, K., & Brazier, R. E. (2019). Assessing the impact of peat erosion on growing season CO<sub>2</sub> fluxes by comparing erosional peat pans and surrounding vegetated hags. *Wetlands Ecology and Management*, 27(2–3), 187–205. <https://doi.org/10.1007/s11273-019-09652-9>
- Gažovič, M., Forbrich, I., Jager, D. F., Kutzbach, L., Wille, C., & Wilmking, M. (2013). Hydrology-driven ecosystem respiration determines the carbon balance of a boreal peatland. *Science of the Total Environment*, 463–464, 675–682. <https://doi.org/10.1016/j.scitotenv.2013.06.077>
- Gerdol, R., & Vicentini, R. (2011). Response to heat stress of populations of two *Sphagnum* species from alpine bogs at different altitudes. *Environmental and Experimental Botany*, 74(1), 22–30. <https://doi.org/10.1016/j.envexpbot.2011.04.010>
- Goud, E. M., Moore, T. R., & Roulet, N. T. (2017). Predicting peatland carbon fluxes from non-destructive plant traits. *Functional Ecology*, 31(9), 1824–1833. <https://doi.org/10.1111/1365-2435.12891>
- Goud, E. M., Touchette, S., Strachan, I. B., & Strack, M. (2021). Graminoids vary in functional traits, carbon dioxide and methane fluxes in a restored peatland: Implications for modeling carbon storage. *Journal of Ecology*, 110(9), 2105–2117. <https://doi.org/10.1111/1010.2021.05.27.445980>
- Granath, G., Moore, P. A., Lukenbach, M. C., & Waddington, J. M. (2016). Mitigating wildfire carbon loss in managed northern peatlands through restoration. *Scientific Reports*, 6(1), 1–9. <https://doi.org/10.1038/srep28498>
- Grau-Andrés, R., Davies, G. M., Gray, A., Scott, E. M., & Waldron, S. (2018). Fire severity is more sensitive to low fuel moisture content on *Calluna* heathlands than on peat bogs. *Science of the Total Environment*, 616–617, 1261–1269. <https://doi.org/10.1016/j.scitotenv.2017.10.192>
- Grillakis, M. G. (2019). Increase in severe and extreme soil moisture droughts for Europe under climate change. *Science of the Total Environment*, 660, 1245–1255. <https://doi.org/10.1016/j.scitotenv.2019.01.001>
- Hancock, M. H., England, B., & Cowie, N. R. (2018). Knockfin Heights: A high-altitude flow country peatland showing extensive erosion of uncertain origin. *Mires and Peat*, 23, 1–20. <https://doi.org/10.19189/MaP.2018.OMB.334>
- Hari, V., Rakovec, O., Markonis, Y., Hanel, M., & Kumar, R. (2020). Increased future occurrences of the exceptional 2018–2019 Central European drought under global warming. *Scientific Reports*, 10(1), 12207. <https://doi.org/10.1038/s41598-020-68872-9>
- Helfter, C., Campbell, C., Dinsmore, K. J., Drewer, J., Coyle, M., Anderson, M., Skiba, U., Nemitz, E., Billett, M. F., & Sutton, M. A. (2015). Drivers of long-term variability in CO<sub>2</sub> net ecosystem

- exchange in a temperate peatland. *Biogeosciences*, 12(6), 1799–1811. <https://doi.org/10.5194/bg-12-1799-2015>
- Hermans, R., Zahn, N., Andersen, R., Teh, Y. A., Cowie, N., & Subke, J. A. (2019). An incubation study of GHG flux responses to a changing water table linked to biochemical parameters across a peatland restoration chronosequence. *Mires and Peat*, 23, 1–18. <https://doi.org/10.19189/MaP.2018.DW.354>
- Hothorn, T., Bretz, F., & Westfall, P. (2008). Simultaneous inference in general parametric models. *Biometrical Journal*, 50, 346–363. <https://doi.org/10.1002/bimj.200810425>
- Huth, V., Vaidya, S., Hoffmann, M., Jurisch, N., Günther, A., Gundlach, L., Hagemann, U., Elsgaard, L., & Augustin, J. (2017). Divergent NEE balances from manual-chamber CO<sub>2</sub> fluxes linked to different measurement and gap-filling strategies: A source for uncertainty of estimated terrestrial C sources and sinks? *Journal of Plant Nutrition and Soil Science*, 180(3), 302–315. <https://doi.org/10.1002/jpln.201600493>
- Huttunen, J. T., Väisänen, T. S., Heikkinen, M., Hellsten, S., Nykänen, H., Nenonen, O., & Martikainen, P. J. (2002). Exchange of CO<sub>2</sub>, CH<sub>4</sub> and N<sub>2</sub>O between the atmosphere and two northern boreal ponds with catchments dominated by peatlands or forests. *Plant and Soil*, 242(1), 137–146.
- Järveoja, J., Nilsson, M. B., Crill, P. M., & Peichl, M. (2020). Bimodal diel pattern in peatland ecosystem respiration rebuts uniform temperature response. *Nature Communications*, 11(1), 1, 4255–9. <https://doi.org/10.1038/s41467-020-18027-1>
- Jassey, V. E. J., & Signarbieux, C. (2019). Effects of climate warming on *Sphagnum* photosynthesis in peatlands depend on peat moisture and species-specific anatomical traits. *Global Change Biology*, 25(11), 3859–3870. <https://doi.org/10.1111/gcb.14788>
- Keane, J. B., Toet, S., Ineson, P., Weslien, P., & Klemetsson, L. (2020). Carbon flux response and recovery to drought years in a hemi-boreal peat bog between different vegetation types. In EGU (13187). EGU General Assembly. <https://ui.adsabs.harvard.edu/abs/2020EGUGA.2213187K/abstract>
- Keiser, A. D., Smith, M., Bell, S., & Hofmocker, K. S. (2019). Peatland microbial community response to altered climate tempered by nutrient availability. *Soil Biology and Biochemistry*, 137, 107561. <https://doi.org/10.1016/j.soilbio.2019.107561>
- Kool, A., & Heijmans, M. M. P. D. (2009). Dwarf shrubs are stronger competitors than graminoid species at high nutrient supply in peat bogs. *Plant Ecology*, 204(1), 125–134. <https://doi.org/10.1007/s11258-009-9574-7>
- Kritzler, U. H., Artz, R. R. E., & Johnson, D. (2016). Soil CO<sub>2</sub> efflux in a degraded raised bog is regulated by water table depth rather than recent plant assimilate. *Mires and Peat*, 17, 1–14. <https://doi.org/10.19189/MaP.2015.OMB.203>
- Kross, A. S. E., Roulet, N. T., Moore, T. R., Lafleur, P. M., Humphreys, E. R., Seaquist, J. W., Flanagan, L. B., & Aurela, M. (2014). Phenology and its role in carbon dioxide exchange processes in northern peatlands. *Journal of Geophysical Research*, G: Biogeosciences, 119(7), 1370–1384. <https://doi.org/10.1002/2014JG002666>
- Kuiper, J. J., Mooij, W. M., Bragazza, L., & Robroek, B. J. M. (2014). Plant functional types define magnitude of drought response in peatland CO<sub>2</sub> exchange. *Ecology*, 95(1), 123–131. <https://doi.org/10.1890/13-0270.1>
- Kutzbach, L., Schneider, J., Sachs, T., Giebels, M., Nykänen, H., Shurpali, N. J., Martikainen, P. J., Alm, J., & Wilking, M. (2007). CO<sub>2</sub> flux determination by closed-chamber methods can be seriously biased by inappropriate application of linear regression. *Biogeosciences*, 4(6), 1005–1025. <https://doi.org/10.5194/bg-4-1005-2007>
- Laine, A., Byrne, K. A., Kiely, G., & Tuittila, E. S. (2007). Patterns in vegetation and CO<sub>2</sub> dynamics along a water level gradient in a lowland blanket bog. *Ecosystems*, 10(6), 890–905. <https://doi.org/10.1007/s10021-007-9067-2>
- Laine, A. M., Wilson, D., Alm, J., Schneider, J., & Tuittila, E. S. (2016). Spatial variation in potential photosynthesis in Northern European bogs. *Journal of Vegetation Science*, 27(2), 365–376. <https://doi.org/10.1111/jvs.12355>
- Lapen, D. R., Price, J. S., & Gilbert, R. (2000). Soil water storage dynamics in peatlands with shallow water tables. *Canadian Journal of Soil Science*, 80(1), 43–52. <https://doi.org/10.4141/S99-007>
- Lenth, R., Singmann, H., Love, J., Buerkner, P., & Herve, M. (2020). *emmeans: Estimated Marginal Means, aka Least-Squares Means*. In R package version 1.15-15 (Vol. 34, Issue 1). <https://doi.org/10.1080/00031305.1980.10483031>
- Li, C., Grayson, R., Holden, J., & Li, P. (2018). Erosion in peatlands: Recent research progress and future directions. *Earth-Science Reviews*, 185, 870–886. <https://doi.org/10.1016/j.earscirev.2018.08.005>
- Lindsay, R. (2010). Peatbogs and carbon: A critical synthesis to inform policy development in oceanic peat bog conservation and restoration in the context of climate change. Report to the RSPB, (January 2010), 315. [https://birdwatch.rspb.org.uk/Images/Peatbogs\\_and\\_carbon\\_tcm9-255200.pdf](https://birdwatch.rspb.org.uk/Images/Peatbogs_and_carbon_tcm9-255200.pdf)
- Lindsay, R., Charman, D. J., Everingham, F., O'Reilly, R. M., Palmer, M. A., Rowell, T. A., & Stroud, D. A. (1988). The Flow Country: The peatlands of Caithness and Sutherland. <https://repository.uel.ac.uk/item/86qqv>
- Lowe, J. A., Bernie, D., Bett, P., Bricheno, L., Brown, S., Calvert, D., Clark, R., Eagle, K., Edwards, T., Frosser, G., & Fung, F. (2018). UKCP18 science overview report. Met Office Hadley Centre.
- Lüdecke, D., Makowski, D., Waggoner, P., & Patil, I. (2020). Package “performance”: Assessment of regression models performance. CRAN.R, 14. <https://doi.org/10.1098/rsif.2017.0213>
- Lund, M., Christensen, T. R., Lindroth, A., & Schubert, P. (2012). Effects of drought conditions on the carbon dioxide dynamics in a temperate peatland. *Environmental Research Letters*, 7(4), 45704. <https://doi.org/10.1088/1748-9326/7/4/045704>
- Marschall, M., & Proctor, M. C. F. (2004). Are bryophytes shade plants? Photosynthetic light responses and proportions of chlorophyll a, chlorophyll b and total carotenoids. *Annals of Botany*, 94(4), 593–603. <https://doi.org/10.1093/aob/mch178>
- Marshall, C., Gilbert, P., Sterk, H. P., Bradley, A., Andersen, R., Parry, L., Sowter, A., Marsh, S., & Large, D. (2019). Peat surface response to the 2018 European drought event. Evidence from InSAR and levelling. *Geophysical Research Abstracts* (Vol. 21).
- Marshall, C., Sterk, H. P., Gilbert, P. J., Andersen, R., Bradley, A. V., Sowter, A., Marsh, S., & Large, D. J. (2022). Multiscale variability and the comparison of ground and satellite radar based measures of peatland surface motion for peatland monitoring. *Remote Sensing*, 14(2), 336. <https://doi.org/10.3390/RS14020336>
- Matsuura, S., Mori, A., Hojito, M., Kanno, T., & Sasaki, H. (2011). Evaluation of a portable chamber system for soil CO<sub>2</sub> efflux measurement and the potential errors caused by internal compensation and water vapor dilution. *Journal of Agricultural Meteorology*, 67(3), 127–137. <https://doi.org/10.2480/agrmet.67.3.7>
- Murphy, J. T., Ham, J. M., & Owensby, C. E. (2014). Design and testing of a novel gas exchange chamber. *Academic Research Journal of Agricultural Science and Research*, 2(July), 34–46. <https://doi.org/10.14662/ARJASR2014.016>
- Nakagawa, S., & Schielzeth, H. (2010). Repeatability for Gaussian and non-Gaussian data: A practical guide for biologists. *Biological Reviews*, 85, 935, no-956. <https://doi.org/10.1111/j.1469-185X.2010.00141.x>
- Nakagawa, S., & Schielzeth, H. (2013). A general and simple method for obtaining R<sup>2</sup> from generalized linear mixed-effects models. *Methods in Ecology and Evolution*, 4(2), 133–142. <https://doi.org/10.1111/j.2041-210x.2012.00261.x>
- Padfield, D., & Matheson, G. (2018). nls.multstart: Robust non-linear regression using AIC scores version 1.1.0 from CRAN. <https://rdrr.io/cran/nls.multstart/>
- Parkinson, K. J. (1981). An improved method for measuring soil respiration in the field. *The Journal of Applied Ecology*, 18, 221. <https://doi.org/10.2307/2402491>
- Pinheiro, J., Bates, D., DebRoy, S., Sarkar, D., & R Core Team. (2020). nlme: Linear and Nonlinear Mixed Effects Models. <https://CRAN.R-project.org/package=nlme>

- Pirk, N., Mastepanov, M., Parmentier, F. J. W., Lund, M., Crill, P., & Christensen, T. R. (2016). Calculations of automatic chamber flux measurements of methane and carbon dioxide using short time series of concentrations. *Biogeosciences*, 13(4), 903–912. <https://doi.org/10.5194/bg-13-903-2016>
- Potvin, L. R., Kane, E. S., Chimner, R. A., Kolka, R. K., & Lilleskov, E. A. (2014). Effects of water table position and plant functional group on plant community, aboveground production, and peat properties in a peatland mesocosm experiment (PEATcosm). *Plant and Soil*, 387(1–2), 277–294. <https://doi.org/10.1007/s11104-014-2301-8>
- Price, J. S. (2003). Role and character of seasonal peat soil deformation on the hydrology of undisturbed and cutover peatlands. *Water Resources Research*, 39(9). <https://doi.org/10.1029/2002WR001302>
- R Core Development Team. (2014). *R: A language and environment for statistical computing*. R Foundation for Statistical Computing. <http://www.R-Project.Org/>
- Radu, D. D., & Duval, T. P. (2018). Precipitation frequency alters peatland ecosystem structure and CO<sub>2</sub> exchange: Contrasting effects on moss, sedge, and shrub communities. *Global Change Biology*, 24(5), 2051–2065. <https://doi.org/10.1111/gcb.14057>
- Robroek, B. J. M., Jassey, V. E. J., Kox, M. A. R., Berendsen, R. L., Mills, R. T. E., Cécillon, L., Puisant, J., Meima-Franke, M., Bakker, P. A. H. M., & Bodelier, P. L. E. (2015). Peatland vascular plant functional types affect methane dynamics by altering microbial community structure. *Journal of Ecology*, 103(4), 925–934. <https://doi.org/10.1111/1365-2745.12413>
- Robroek, B. J. M., Jassey, V. E. J., Payne, R. J., Martí, M., Bragazza, L., Bleeker, A., Buttler, A., Caporn, S. J. M., Dise, N. B., Kattge, J., Zając, K., Svensson, B. H., van Ruijven, J., & Verhoeven, J. T. A. (2017). Taxonomic and functional turnover are decoupled in European peat bogs. *Nature Communications*, 8(1), 1161.
- Roudier, P., Andersson, J. C. M., Donnelly, C., Feyen, L., Greuell, W., & Ludwig, F. (2016). Projections of future floods and hydrological droughts in Europe under a +2°C global warming. *Climatic Change*, 135(2), 341–355. <https://doi.org/10.1007/s10584-015-1570-4>
- Saunders, M., Ingle, R., & Regan, S. (2021). Assessing the impact of exceptional inter-annual climatic variability on rates of net ecosystem carbon dioxide exchange at Clara bog. In *EGU General Assembly Conference Abstracts* (pp. EGU21–13414).
- Seabold, S., & Perktold, J. (2010). Statsmodels: Econometric and statistical modeling with Python. In *Proceedings of the 9th Python in science conference* (pp. 92–96). <http://statsmodels.sourceforge.net/>
- SNH. (2016). Carbon and Peatland Map. Scottish Natural Heritage. 2016. <http://soils.environment.gov.scot/maps/thematic-maps/carbon-and-peatland-2016-map/>
- Silva, J. P., Lasso, A., Lubberding, H. J., Peña, M. R., & Gijzen, H. J. (2015). Biases in greenhouse gases static chambers measurements in stabilization ponds: Comparison of flux estimation using linear and non-linear models. *Atmospheric Environment*, 109, 130–138. <https://doi.org/10.1016/j.atmosenv.2015.02.068>
- Smart, P. J. (1982). Stratigraphy of a site in the Munsary Dubh Lochs, Caithness, Northern Scotland: Development of the present pattern. *The Journal of Ecology*, 70(2), 549. <https://doi.org/10.2307/2259922>
- Sottocornola, M., & Kiely, G. (2005). An Atlantic blanket bog is a modest CO<sub>2</sub> sink. *Geophysical Research Letters*, 32(23), 1, L23804–4. <https://doi.org/10.1029/2005GL024731>
- Sterk, H. P., Detrey, I., Marshall, C., Cowie, N. R., Payne, R., McIlvenny, J., & Andersen, R. (2019). Capturing gas fluxes on your phone: An iOS- and Android-based data-logging setup for EGM-4 environmental gas monitoring systems. *Journal of Environmental Quality*, 48(5), 1557–1560. <https://doi.org/10.2134/jeq2019.04.0163>
- Strachan, I. B., Pelletier, L., & Bonneville, M. C. (2016). Inter-annual variability in water table depth controls net ecosystem carbon dioxide exchange in a boreal bog. *Biogeochemistry*, 127(1), 99–111. <https://doi.org/10.1007/s10533-015-0170-8>
- Strack, M., Cagampan, J., & Hassanpour Fard, G. (2016). Controls on plot-scale growing season CO<sub>2</sub> and CH<sub>4</sub> fluxes in restored peatlands: Do they differ from unrestored and natural sites? *Mires and Peat*, 17(05), 1–18. <https://doi.org/10.19189/MaP.2015.OMB.216>
- Strack, M., Waddington, J. M., Lucchese, M. C., & Cagampan, J. P. (2009). Moisture controls on CO<sub>2</sub> exchange in a *Sphagnum*-dominated peatland: Results from an extreme drought field experiment. *Ecohydrology*, 2(4), 454–461. <https://doi.org/10.1002/eco.68>
- Swenson, M. M., Regan, S., Bremmers, D. T. H., Lawless, J., Saunders, M., & Gill, L. W. (2019). Carbon balance of a restored and cutover raised bog: Implications for restoration and comparison to global trends. *Biogeosciences*, 16(3), 713–731. <https://doi.org/10.5194/bg-16-713-2019>
- Tampuu, T., Praks, J., Uiboupin, R., & Kull, A. (2020). Long term interferometric temporal coherence and DInSAR phase in northern peatlands. *Remote Sensing*, 12(10), 1566. <https://doi.org/10.3390/rs12101566>
- Turetsky, M. R. (2003). The role of bryophytes in carbon and nitrogen cycling. *The Bryologist*, 106(3), 395–409. <https://doi.org/10.1639/05>
- Turner, T. E., Billett, M. F., Baird, A. J., Chapman, P. J., Dinsmore, K. J., & Holden, J. (2016). Regional variation in the biogeochemical and physical characteristics of natural peatland pools. *Science of the Total Environment*, 545–546, 84–94. <https://doi.org/10.1016/j.scitotenv.2015.12.101>
- van Breemen, N. (1995). How *Sphagnum* bogs down other plants. *Trends in Ecology & Evolution*, 10(7), 270–275. [https://doi.org/10.1016/0169-5347\(95\)90007-1](https://doi.org/10.1016/0169-5347(95)90007-1)
- Wagner, S. W., Reicosky, D. C., & Alessi, R. S. (1997). Regression models for calculating gas fluxes measured with a closed chamber. *Agronomy Journal*, 89(2), 279–284. <https://doi.org/10.2134/agnonj1997.00021962008900020021x>
- Ward, S. E., Bardgett, R. D., McNamara, N. P., & Ostle, N. J. (2009). Plant functional group identity influences short-term peatland ecosystem carbon flux: Evidence from a plant removal experiment. *Functional Ecology*, 23(2), 454–462. <https://doi.org/10.1111/j.1365-2435.2008.01521.x>
- Wickham, H., Chang, W., Henry, L., Pedersen, T. L., Takahashi, K., Wilke, C., & Woo, K. (2019). ggplot2: Create elegant data visualisations using the grammar of graphics. 2018. Cran-R Project.
- Widén, B., & Lindroth, A. (2003). A calibration system for soil carbon dioxide-efflux measurement chambers. *Soil Science Society of America Journal*, 67(1), 327–334. <https://doi.org/10.2136/sssaj2003.3270>
- Wilson, D., Alm, J., Riutta, T., Laine, J., Byrne, K. A., Farrell, E. P., & Tuittila, E. S. (2007). A high resolution green area index for modelling the seasonal dynamics of CO<sub>2</sub> exchange in peatland vascular plant communities. *Plant Ecology*, 190(1), 37–51. <https://doi.org/10.1007/s11258-006-9189-1>
- Wilson, D., Farrell, C. A., Fallon, D., Moser, G., Müller, C., & Renou-Wilson, F. (2016). Multiyear greenhouse gas balances at a rewetted temperate peatland. *Global Change Biology*, 22(12), 4080–4095. <https://doi.org/10.1111/gcb.13325>
- Wood, S. N. (2017). *Generalized additive models: An introduction with R* (2nd ed.). Chapman and Hall/CRC. <https://doi.org/10.1201/9781315370279>

## SUPPORTING INFORMATION

Additional supporting information can be found online in the Supporting Information section at the end of this article.

**How to cite this article:** Sterk, H. P., Marshall, C., Cowie, N. R., Clutterbuck, B., McIlvenny, J., & Andersen, R. (2022). Blanket bog CO<sub>2</sub> flux driven by plant functional type during summer drought. *Ecohydrology*, e2503. <https://doi.org/10.1002/eco.2503>